C.P. No. 526 C.P. No. 526

MINISTRY OF AVIATION

AERONAUTICAL RESEARCH COUNCIL

CURRENT PAPERS

The Performance of a Cascade Fitted with Blown Flaps

By

R.A. Kruger, H. Marsh and J.H. Horlock

Engineering Department, University of Cambridge

LONDON: HER MAJESTY'S STATIONERY OFFICE

1961

FIVE SHILLINGS NET

ERRATA

(i) On page 3, line 17, read Γ_k at $Z_k \pm i\lambda s$

(ii) On page 3, Eqn.(12) et seq., read $\coth\left[\frac{\pi(Z-Z_k)}{s}\right]$

for $\cot h\left[\frac{\pi(Z-Z_k)}{s}\right]$

(iii) In Appendix I, read

c_j jet coefficient $= \frac{\rho_j v_j^2 b}{\frac{1}{2}\rho U_o^2 s}$

c_L lift coefficient $= \frac{L}{\frac{1}{2}\rho U_o^2 s}$

J jet momentum $= \rho_j v_j^2 b$

(iv) In Appendix II, for Eqn.(4) read $\frac{d}{d\ell}(Av_1) + bv_j = 0$

(v) In Fig.3b, the dimensions are s = 6", c_f = 5", f = 1" and c = 6"

(vi) In Figs.5 to 10, the velocity U should read U_o.

C.P. No.526

The Performance of a Cascade Fitted with Blown Flaps

- By -
R. A. Kruger, H. Marsh and
J. H. Horlock
(formerly Engineering Department,
University of Cambridge)

23rd June, 1959

1. Introduction

The axial flow compressor of a gas turbine engine is often required to operate at mass flow rates and rotational speeds well below those for which it was designed. Under such conditions, the front stages of the compressor may stall and various mechanisms may be used in order to delay this stalling (and the consequent surging of the compressor) to lower speeds. Inlet guide vanes may be used; the deflection through the inlet guide vanes is increased at lower rotational speeds, and the incidence on to the first stage rotor is reduced. Alternatively, an air flow greater than that delivered by the compressor may be passed through the front stages and the excess air bled off from some intermediate stage in the compressor. These two methods (variable stagger guide vanes and bleeding) are often combined to give better "off-design" performance. Further a system for recirculating the bled air has been proposed: the stall of the first stage rotor may be prevented by the increase in local axial velocity resulting from injection of the bled air into the main stream ahead of the first stage.

A range of high lift coefficients has been obtained on an isolated aerofoil by using a "jet flap" arrangement in which a high velocity jet sheet is discharged from the lower surface of the aerofoil into the main stream (Davidson, 1956). Stratford (1956) has also described experiments in which the jet is blown from the upper surface of the aerofoil over a mechanical flap. This construction, a "blown flap", has the advantage that the jet discharge angle is easily altered; the mechanical flap angle may be changed quickly and the jet follows the flap up to large flap angles.

The present investigation was made to study the performance of a cascade of inlet guide vanes fitted with blown flaps. In an axial flow compressor, the air discharged over such blown flaps might come from the recirculated bled air. The deflection through the guide vanes would be determined by the momentum flux of the jet and such a system would combine the advantages of "recirculation bleed" and variable stagger guide vanes without the mechanical complications of variable stagger.

A series of experiments with a cascade of uncambered blades fitted with blown flaps is reported. The flap angle was varied from 15° to 60° and a range of jet coefficients, c_j, of 0.0 to 0.4 was used. With this range of jet coefficients a maximum variation in the deflection, ϵ, of 13.5° was obtained at a flap angle of 45°. If variations of this magnitude can be obtained without adversely affecting the operation of the compressor at design conditions then equipping the inlet guide vanes with either "blown flaps" or "jet flaps" might be worthwhile.

An/

An analytical method is presented for estimating the performance of a cascade of blades fitted with "blown flaps" and fair agreement with the experimental behaviour is obtained when the cascade is unstalled.

2. Linearised Analysis

Linearised analyses of the flow past an isolated aerofoil with a jet flap have been given by Spence (1953) and Ross and Davies (1957). Spence (1958) has since given an analysis for an aerofoil fitted with a blown flap. In the linearised analysis given below for a cascade of aerofoils fitted with blown flaps, the blades and jets are replaced by vortex sheets. Two vortex sheets (Fig. 1a) replace the thin parallel sided jet, and have the property of transmitting the jet.

A mathematical model of the cascade flow is shown in Figs. 1(a) and (b). Davidson (1956), Spence (1956) and Ross and Davies (1957) have described how the curvature of the jet will require a pressure difference across it; if the strengths of the vortex sheets separating the jet from the mainstream, or from the blade, (as at A in Fig. 1a) are γ_1 and γ_2 per unit length, then for the flow downstream from the blade,

$$\gamma_1 + \gamma_2 = \frac{J \cos \theta}{\rho U_o R} \qquad \ldots(1)$$

$$= \tfrac{1}{2}\, c_j s\, U_o \cos \theta \frac{d\theta}{d\xi}. \qquad \ldots(2)$$

On the blade at A

$$\gamma_1 + \gamma_2 = U^1 \qquad \ldots(3)$$

where U^1 is the local free stream velocity.

If the flow follows the flap, the strength of the vortex sheet representing the blade and the jet flow over the blade will be the same as when the jet is discharged from the trailing edge in the direction of the flap.

If the vortex sheets representing the jets are replaced by discrete vortices, then from integration of equation (2)

$$\Gamma_k = \tfrac{1}{2}\, c_j s\, U_o(\sin \theta_n - \sin \theta_{n-1}) \qquad \ldots(4)$$

where

$$\Gamma_k = \int_{\xi_{n-1}}^{\xi_n} (\gamma_1 + \gamma_2) d\xi. \qquad \ldots(5)$$

The total circulation around the jet can be obtained by integrating equation (2) along the length of the jet to give,

$$\Gamma_{jet} = \tfrac{1}{2}\, c_j s\, U_o(\sin \tau - \sin \epsilon). \qquad \ldots(6)$$

(This equation can also be obtained directly by relating the "lift" on the jet to its change of momentum in the y direction.)

If at the trailing edge, the pressure is the same on both sides of the jet, (i.e., there is no curvature of the jet), then the lift per unit length experienced by the aerofoil is,

L/

$$L = \rho U_o \Gamma_{aerofoil} + J \sin \tau \qquad \ldots(7)$$

$$= \rho U_o (\Gamma_{aerofoil} + \tfrac{1}{2} c_j s U_o \sin \tau) \qquad \ldots(7a)$$

where $\Gamma_{aerofoil}$ is the total circulation around the aerofoil.

Substituting for $(\frac{1}{2} c_j s U_o \sin \tau)$ from equation (6)

$$L = \rho U_o(\Gamma_{aerofoil} + \Gamma_{jet} + \tfrac{1}{2} c_j s U_o \sin \epsilon) \qquad \ldots(8)$$

$$= \rho U_o(\Gamma_{total} + \tfrac{1}{2} c_j s U_o \sin \epsilon). \qquad \ldots(8a)$$

If the momentum flux through the control surface shown in Fig. 2a is now considered, then

$$L = \rho U_o^2 s \tan \epsilon + J \sin \epsilon \qquad \ldots(9)$$

$$= \rho U_o(U_o s \tan \epsilon + \tfrac{1}{2} c_j s U_o \sin \epsilon) \qquad \ldots(9a)$$

or

$$C_L = \frac{s}{C} (2 \tan \epsilon + c_j \sin \epsilon). \qquad \ldots(10)$$

Comparing equations (8a) and (9a)

$$\tan \epsilon = \frac{\Gamma_{total}}{sU_o} \qquad \ldots(11)$$

which relates the final air angle to the total circulation around aerofoil and jet.

If the aerofoils and jets are now represented by a number of columns of discrete vortices, Γ_k at $Z \pm i\lambda s$ where $\lambda = 0, 1, 2 \ldots,$ then the conjugate complex velocity is given by

$$w = u - iv = U_o + \frac{i}{2s} \sum \Gamma_k \left(1 + \coth \left[\frac{\pi(Z-Z_k)}{s}\right]\right) \qquad \ldots(12)$$

where U_o is the uniform velocity far upstream.

From this equation, the direction of flow far downstream from the cascade is

$$\tan \epsilon = \frac{\Sigma\Gamma_k}{sU_o}$$

which is in agreement with equation (11).

If, as in Fig. 3a, the aerofoil and jet are replaced by eight discrete vortices, then we have the following set of equations for the flow field,

$$u_n - iv_n = U_o + \frac{i}{2s}\sum_1^8 \Gamma_k\left[1 + \cot h\left(\frac{\pi(Z_n - Z_k)}{s}\right)\right]$$

for all values of n, with the conditions

$$v_n = 0, \text{ for } n = 1, 2, 3$$

$$v_n = -U_n \tan \tau, \text{ for } n = 4$$

$$\Gamma_k = \tfrac{1}{2} c_j s\, U_o(\sin \theta_n - \sin \theta_{n-1})$$

$$\text{for } n = 5, 6, 7, 8$$

$$\tan \theta_n = \frac{(v_n)}{(u_n)}, \text{ for all n.}$$

$$\tan \epsilon = \frac{1}{sU_o}\sum_1^8 \Gamma_k$$

and $\epsilon = \theta_8$. (A)

A numerical solution of these equations has not yet been obtained for the case when the flap angle is large. When the flap angle is small, the vortices in the jet can be approximated by vortices on the x axis and the conditions of equations (A) may be applied at the corresponding points on the x axis. The flow at these points is then parallel to the jet and equations (A) reduce to

$$u_n - iv_n = U_o + \frac{i}{2s}\sum_1^8 \Gamma_k\left[1 + \cot h\left(\frac{\pi(x_n - x_k)}{s}\right)\right]$$

for all values of n, with the conditions

$$v_n = 0, \text{ for } n = 1, 2, 3$$

$$v_n = -U_o \tau, \text{ for } n = 4$$

$$\Gamma_k = \tfrac{1}{2} c_j s\, U_o(\theta_n - \theta_{n-1}), \text{ for } n = 5, 6, 7, 8$$

$$\theta_n = \frac{v_n}{U_o} \text{ for all n}$$

and $\epsilon = \frac{1}{sU_o}\sum_1^8 \Gamma_k$. (B)

The numerical solution of these equations (obtained using a digital computer) shows that with $c_j \leq 0.9$, the vorticity in the jet is small and mainly concentrated in the first of the four jet vortices. Since the vorticity in the jet is always of the same sign, a further simplification may be made in which each blade is represented by three vortices and the total vorticity in the jet is replaced by a single vortex Γ_4. For this analysis, a fixed point at a distance of 1" (s/6) along the extrapolated flap line was chosen as the position of Γ_4. (The solution is not sensitive to the position of Γ_4.)

With the simple model shown in Fig.3(b), the analysis need not be restricted to very small flap angles and equations (A) are then

$$\left.\begin{aligned} u_n - iv_n &= U_o + \frac{i}{2s}\sum_1^4 \Gamma_k\left[1 + \coth\left(\frac{\pi(Z_n-Z_k)}{s}\right)\right] \\ &\text{for all } n, \text{ with the conditions} \\ v_n &= 0, \text{ for } n = 1, 2 \\ v_n &= -u_n \tan\tau, \quad \text{for } n = 3 \\ \Gamma_4 &= \tfrac{1}{2} c_J s\, U_o(\sin\tau - \sin\epsilon) \\ \text{and} \quad \tan\epsilon &= \frac{1}{sU_o}\sum_1^4 \Gamma_k. \end{aligned}\right\} \quad (C)$$

When the flap angle is small and $0 \leqslant c_J \leqslant 1.0$, the values of ϵ/τ derived from equations (C) are about 2 to 3% less than the values obtained from equations (B).

The performance of the two cascades described in this report, was estimated from this four vortex model and it was found that when the cascade was unstalled, there was close agreement with the experimental results.

3. Apparatus and Instrumentation

The apparatus used in these tests consisted of five major elements. These were the wind tunnel, the cascade with blown flaps, the jet air supply, the probe used for the survey of the wake and the associated instrumentation. The general arrangement of the apparatus is shown in Figs.4(a) and (b).

The 150 hp wind tunnel in the Cambridge University Engineering Laboratory (Rhoden, 1950) was used with blades of six inch chord and eighteen inch length. An upstream velocity of 50 ft/sec was used in most of the tests. This velocity was sufficiently low to allow jet coefficients of 0.4 to be obtained with the jet air supply available. A few experiments were made at lower tunnel speeds in order to obtain higher jet coefficients.

Because of the difficulty in providing large flow rates using air of high total pressure, it was necessary to limit the number of blades with blown flaps to three. This introduced non-uniformities along the cascade in the flow downstream.

Since a major object of these experiments was to examine the performance of a cascade with varying jet discharge angles, blown flaps were used rather than jet flaps. Stratford (1956) has shown that blowing a jet sheet over a movable mechanical flap is an effective method of simulating a jet flap with a variable initial angle. The initial tests were made with flaps of one inch chord and later, a second series of tests were made with flaps of one half inch chord.

The problem of distributing the air supply along the length of the blade to give a uniform jet sheet is discussed in Appendix II. Manifolds of the type described were used in the construction of the cascade.

In order to measure the static pressure distributions over the surface of the centre blade, the blade and the one inch flap were equipped with pressure tappings. A total of 29 pressures were measured at a maximum chord spacing of one half inch.

The/

The air supply for the jets was provided by two fans operating in series to produce a head of fifty inches of water at the flow rate required. The fans supplied a large settling chamber upstream of the manifolds. The flow in the ducts was controlled to ensure equal division of the air supply between the three blades. In order to calculate the jet coefficient, c_j, pressure measurements were made at the entry sections to the manifolds and the temperature in the settling chamber was measured.

The pressure distributions in the wake were measured with a probe mounted on a mechanism to measure vertical displacement and angle of rotation. The probe was constructed from four lengths of nickel tubing (I.D. = 0.0735"); two of these formed the yaw meter and the other two were used to measure the total and static pressures.

Several other measurements were made in order to calculate the tunnel velocity and flow rate. These were the total and static pressures measured upstream of the cascade, the temperature of the tunnel flow and the ambient pressure.

4. Discussion of Experimental Results

4.1 Preliminary experiments

A number of preliminary experiments were made in order to calibrate and determine the errors in the apparatus. The first was to find the critical Reynolds number corresponding to a sudden increase in the total pressure loss across the cascade. With no jet flow and no flap angle, this occurred at a tunnel velocity of about 40 ft/sec. With jet flow and a positive flap angle, τ, the critical velocity will be lower than 40 ft/sec. A tunnel velocity of 50 ft/sec was therefore used for most of the tests. A few tests were carried out at lower tunnel speeds in order to obtain higher values of the jet coefficient.

A manifold, similar to those used in the cascade, was tested separately to determine the variation in the jet velocity with distance along the blade. The maximum variation was found to be about 8% and, at the mid span position, the jet velocity was about 3% greater than the mean velocity. The value of the jet coefficient, c_j, was calculated from measurements made in the entry section to the manifolds. A uniform jet velocity was assumed and the calculated value may therefore differ slightly from the value at the mid span position, where the wake surveys were taken.

The flow over the hinge and along the flap was examined by fixing a few tufts of goosedown on to the central blade and flap. The flap was set at 45° and the jet coefficient was varied over the range 0.0 to 0.9. At the higher values of c_j, the Coanda effect was observed and the jet followed the flap. Under these conditions the mathematical model may be a good approximation to the flow through the cascade.

However, at low values of c_j, separation occurred and the jet no longer flowed along the full length of the flap. Under such conditions the model is no longer a good representation of the flow and agreement between the estimated and experimental results should not be expected at low values of c_j.

4.2 Initial tests with 1 inch flaps

The first series of tests were made with flaps of 1 inch chord, the fixed chord length of the blades being 5 inches. The flap angle was varied from 15° to 60° and values of c_j from 0.0 to 0.4 were used.

The static pressure distribution around the central blade was measured and Figs. 5 and 6 show typical pressure distributions. In the

first/

first experiment (Fig. 5) the jet coefficient was not sufficiently high to ensure that the jet flowed along the whole length of the flap. With only a small increase in the jet momentum this condition was obtained and the pressure distribution is shown in Fig. 6. The high suction peak of this curve is caused by the jet flowing over the oblique angle formed by the blade and the flap. The lift coefficient c_{L1} was calculated by integrating the pressure distribution curves and, since the jet is discharged axially (i.e., along the x axis in Fig. 1(a)), no additional term for the jet momentum is required in the calculation of the lift coefficient.

A traverse of the wake was made at 0.3 inch behind the trailing edge. The wake surveys shown in Figs. 7 and 8 correspond to the pressure distributions given in Figs. 5 and 6. In the first experiment (Fig. 7) the jet does not follow the flap and mixes with the mainstream. With a small increase in the jet coefficient a different flow pattern is established. The jet now follows the flap, remaining well defined as shown in Fig. 8. It is only under these conditions that agreement with the analysis may be expected. The lift coefficient, c_{L2}, was calculated from the results of the wake surveys by considering the momentum flux through the control surface shown in Fig. 2(b).

The final air angle, ϵ, cannot be measured directly and it was calculated by measuring the lift coefficient and then using equation (10) of the analysis.

The lift coefficients, c_{L1} and c_{L2}, and the corresponding final air angles, ϵ_1 and ϵ_2, are shown in Figs. 11 to 18, where they may be compared with the solutions of the linearised analysis.

4.3 Second series of tests with 0.5 inch flaps

With the 1 inch flaps, there was a considerable lift with no jet flow, which was due to the effect of the unblown mechanical flap. The second series of tests was made in an attempt to reduce this effect and to approach more closely to the pure 'jet flap'. The tests were made with blades having a fixed chord length of 5 inches and a 0.5 inch blown mechanical flap.

With such small flaps, pressure tappings could not be fitted in the flap and the lift coefficient could only be calculated from the wake surveys made at 0.8 inch behind the trailing edge. Figs. 9 and 10 show two typical wake surveys having the same jet coefficient, but different flap angles. As the flap angle is increased, the jet momentum required to prevent separation also increases. A comparison between Figs. 8 and 10 show that for a given flap angle, the longer flaps require a lower jet coefficient in order that the jet may follow the flap.

The lift coefficient, c_{L2}, and the final air angle, ϵ_2, are shown in Figs. 19 to 24 along with the solutions of the linearised analysis for the 0.5 inch flaps.

4.4 Tests with high jet coefficients

With the shorter flaps set at an angle of 30°, two further tests were made at jet coefficients of 0.65 and 0.90, and the values of c_{L2} and ϵ_2 obtained are shown in Figs. 21 and 22. These higher jet coefficients could only be obtained by lowering the tunnel velocity below the initially determined critical velocity for no jet flow and no flap angle. It is probable, however, that the lowest velocity of 33 ft/sec was still above the critical velocity for that flap angle and jet flow rate.

5./

5. Discussion

In comparisons between the solutions of the linearised analysis and the experimental results, as shown in Figs.11 to 24, the limitations of the apparatus should not be overlooked. One of the main sources of discrepancy is that only three of the six blades in the cascade were fitted with blown flaps, the other three having standard C4 profiles with no camber. The effect of the standard blades is to produce deviations from the flow field for an infinite cascade with blown flaps. However, these deviations are probably a minimum within the vicinity of the central flapped blade. The close agreement between the predicted values of c_L and the values calculated from the pressure distributions, suggests that this is correct.

Away from the central blade, the effect of the uncambered blades may be considerable. From the tests, it was found that the angle of flow at the mid-pitch point on one side of the blade was less than that at the corresponding point on the other side of the blade. With flap angles of 15° and 30°, this difference was about 1.5° or about 10% of the angle measured. When the flap angle was increased to 45° or 60°, the difference increased rapidly to about 4.5° or about 20% of the angle measured. With differences in flow angle of this magnitude, close agreement with the analysis should not be expected for large flap angles. Fig.21 shows that with a flap angle of 30°, there is fair agreement with the analysis, both in the values of c_L and $\frac{\partial c_L}{\partial c_j}$ calculated from the wake surveys.

In the analysis it is assumed that for all values of c_j the flow at the trailing edge is in the direction of the flap. This assumption is only valid for values of the jet coefficient greater than some critical value, c_{js} say, which is dependent on the flap angle and the cascade geometry. For values of c_j less than c_{js} the cascade is stalled and the values of lift coefficient and final air angle are far lower than the estimated values.

The tests indicate that for a given value of c_j, the range of flap angles for an unstalled cascade is less with the shorter flaps. Fig.8 shows that with the 1 inch flaps set at 45° the cascade is unstalled with a jet coefficient of 0.2. Under the same conditions, the cascade with 0.5 inch flaps is stalled, and remains stalled even when c_j is increased to 0.4. A similar comparison may be made when the flap angle is 30°.

The variation of c_{js} with flap angle for an infinite cascade cannot be derived from these results because the presence of the uncambered blades will affect the stalling characteristics of the cascade.

6. Conclusions

The maximum variation of deflection with jet coefficient ($\Delta\epsilon = 13.5°$ for $0 < c_j < 0.4$) was obtained with a flap angle of 45°. The maximum deflection is achieved with a ratio of jet velocity to main stream velocity of approximately 4.5 : 1 and a ratio of jet mass flow to mainstream mass flow of 1 : 22. The variation of deflection with jet coefficient is less if the unstalled region alone is considered. ($\Delta\epsilon = 2.5°$ for $0.2 < c_j < 0.4$).

The observed variation of c_L with c_j in this unstalled region is $0.17/0.2 = 0.85$. At large c_J, $\epsilon \to \tau$ and equation (10) shows that $(dc_L/dc_J) = s/c \sin\tau = 0.707$ in this case.

The variation of lift coefficient with jet coefficient is low for the cascade tested because of the large lift coefficient produced by the mechanical flap alone ($c_J = 0$). A greater variation of lift coefficient and deflection with jet coefficient would be obtained with a

pure/

pure jet flap cascade, and further experiments with such a cascade would be worthwhile. The absolute value of the lift coefficient is smaller than the values obtained with isolated aerofoils (Davidson 1956) because of the smaller change in direction of the jet stream in the cascade. In the isolated aerofoils case the jet must return to the undisturbed free stream direction. In cascades, the jets are finally parallel to the deflected air stream, and their changes of direction (and the associated jet vorticity) are smaller.

Acknowledgements

The authors are indebted to Mr. I. M. Davidson for initial advice on the project, and to Dr. D. S. Whitehead and Miss G. Christ for their assistance in obtaining the analytical solutions.

References

No.	Author(s)	Title, etc.
1	I. M. Davidson	The Jet Flap. Journal of the Royal Aeronautical Society, January, 1956.
2	W. D. Dow	The uniform distribution of a fluid flowing through a perforated pipe. Journal of Applied Mechanics, December, 1950.
3	J. H. Horlock	An investigation of the flow in manifolds with open and closed ends. Journal of the Royal Aeronautical Society, November, 1956.
4	E. Pistolesi	On the calculation of an infinite cascade of thin aerofoils. L'Aerotecchnica V.17, 1937.
5	A. J. Ross and H. J. Davies	A jet deflected from the lower surface of an aerofoil. The Quarterly Journal of Mathematics and Applied Mechanics. August, 1957.
6	D. A. Spence	The lift coefficient of a thin jet-flapped wing. Proc. Roy. Soc. 1956.
7	A. J. Shapiro	The dynamics and thermodynamics of compressible fluid flow. 1953.
8	B. S. Stratford	Early thoughts on the jet flap. Aeronautical Quarterly, February, 1956.
9	B. S. Stratford	Mixing and the jet flap. Aeronautical Quarterly, May, 1956.
10	B. S. Stratford	A further discussion on mixing and the jet flap. Aeronautical Quarterly, August, 1956.

APPENDIX I/

APPENDIX I

Nomenclature

A	cross sectional area of the manifold
b	mean jet slot width
c	total chord length $(c = c_f + f)$
c_f	fixed chord length
c_j	jet coefficient $= \dfrac{(\rho j v^2 j b)}{(\frac{1}{2}\rho U^2 s)}$
c_L	lift coefficient $= \dfrac{(L)}{(\frac{1}{2}\rho U^2 s)}$
f	flap length
J	jet momentum $= \rho_j v_j b$
ℓ	length of blade
L	lift
p	pressure
R	radius of curvature of the jet path
s	vertical distance between the blades
u	velocity component in the x direction
U_o	uniform velocity far upstream
v	velocity component in the y direction
w	conjugate complex velocity $= u - iv$
x	horizontal distance
y	vertical distance
Z	complex variable $= x + iy$
γ	circulation per unit length (clockwise)
Γ	circulation (clockwise)
$\Gamma_{aerofoil}$	total circulation around the aerofoil and the jet flowing over the aerofoil
Γ_{jet}	total circulation around the jet downstream from the trailing edge
ϵ	final air angle
θ	$\tan^{-1}\left(\dfrac{dy}{dx}\right)$
ξ	distance measured along the jet
ρ	density far upstream
ρ_j	density in the jet
τ	flap angle.

APPENDIX II/

APPENDIX II

Manifold Theory

Horlock (1956) has discussed the problem of flow in manifolds with open and closed ends. In the jet flap cascade, it is desired to have a constant momentum flux along the length of the jet sheet. If the Mach number within the manifold is small, then the air may be considered to be an incompressible fluid. If we neglect the effect of friction, then

$$A\cdot\frac{dp_1}{d\ell} + \frac{d}{d\ell}(A\rho v_1^2) = 0 \qquad \ldots(1)$$

and

$$\frac{d}{d\ell}(\tfrac{1}{2}\rho v_j^2) = \frac{d}{d\ell}(p_1 - p_o) \qquad \ldots(2)$$

where p_1 is the static pressure inside the manifold, p_o the exhaust static pressure, which is constant. If

$$\frac{d}{d\ell}(v_j) = 0$$

then $\frac{dp_1}{d\ell} = 0$ from equation (2) and from equation (1) we have

$$\frac{d(Av_1^2)}{d\ell} = 0. \qquad \ldots(3)$$

The continuity equation is

$$\frac{d}{d\ell}(AV_1) + v_j b = 0. \qquad \ldots(4)$$

From these equations the area variation along the length of the manifold (overall length L) is obtained

$$A = A_o\left(\frac{\ell}{L} - 1\right)^2 \qquad \ldots(5)$$

where A_o is the entry area.

Dow (1950) has found experimentally that a linear variation in area produces a substantially uniform velocity of discharge from the manifold. Manifolds of this type were used in the construction of the cascade. With a maximum Mach number of 0.22 in the manifold, the frictional effects were small and a linear variation in the cross-sectional area was adequate.

FIGS. 1a & 1b.

Fig. 1a.

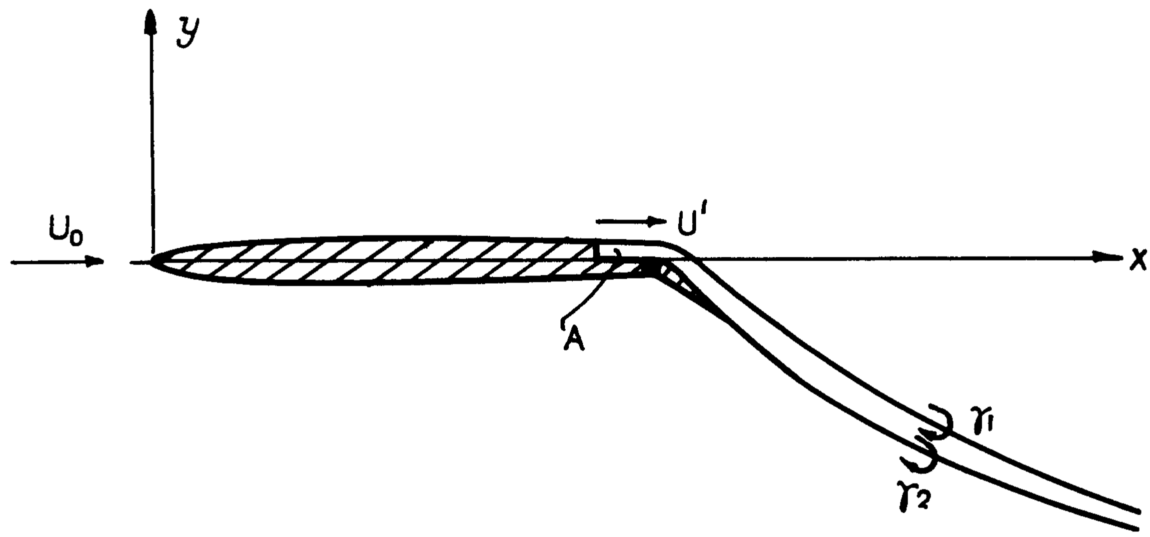

Fig. 1b.

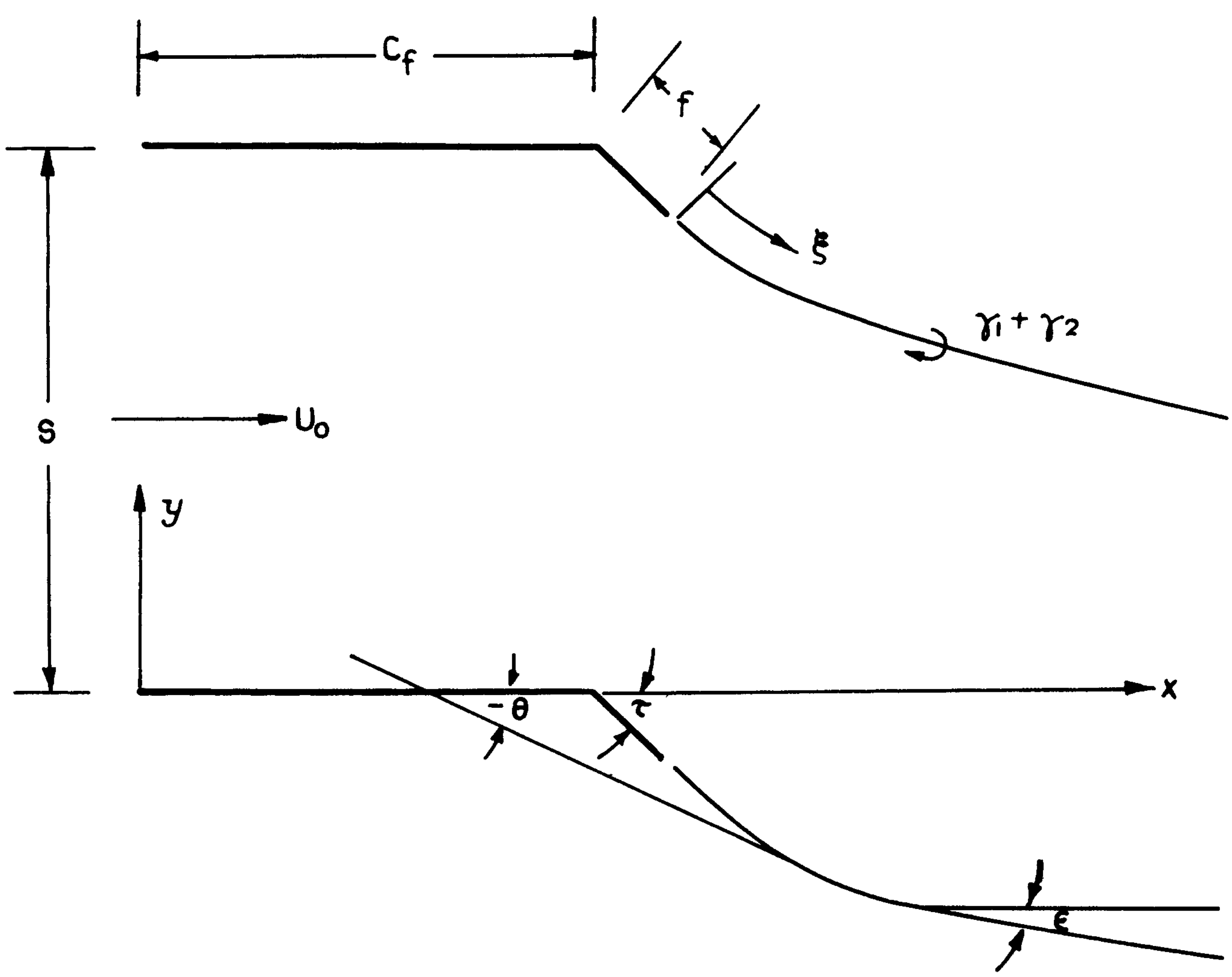

FIGS. 2a & 2b.

FIG. 2a.

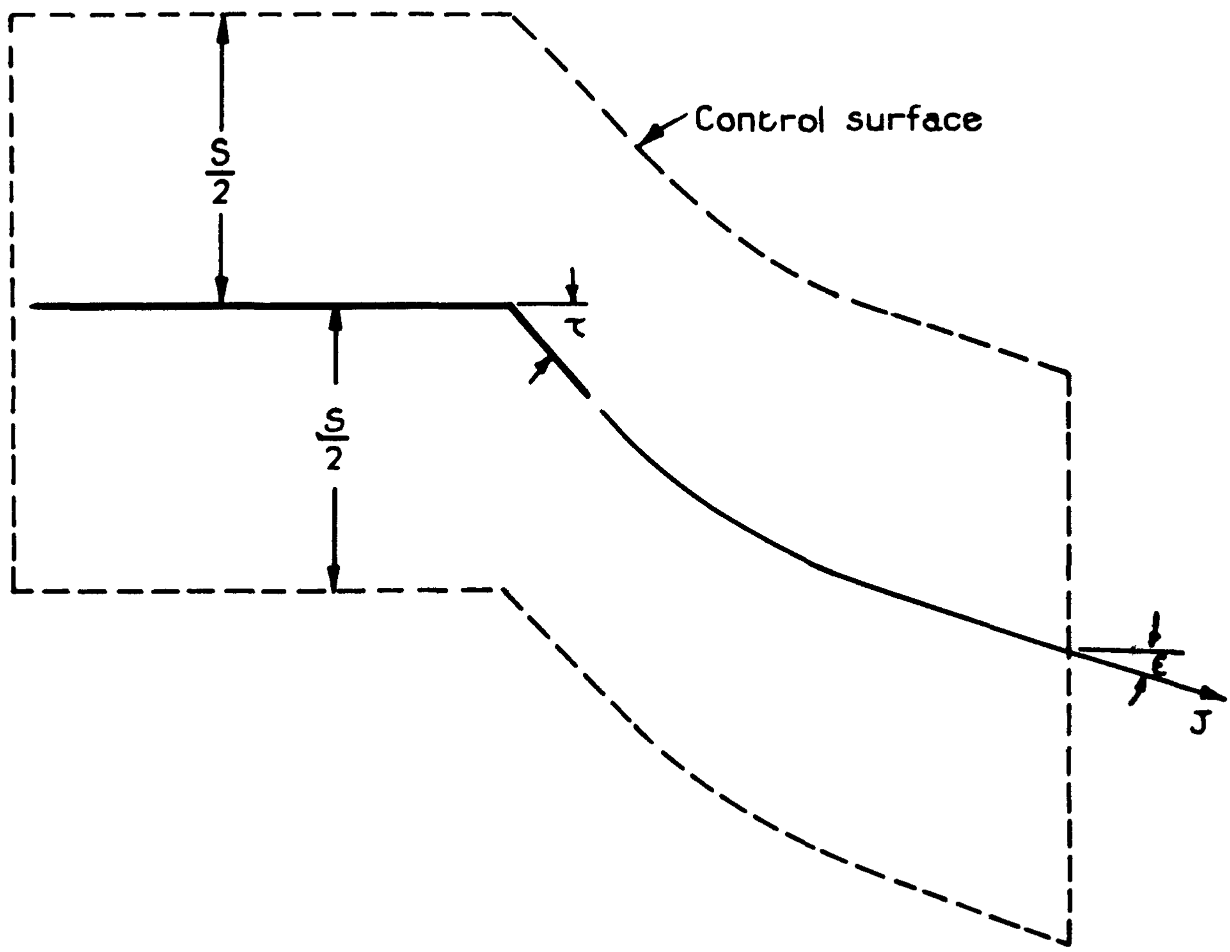

FIG. 2b.

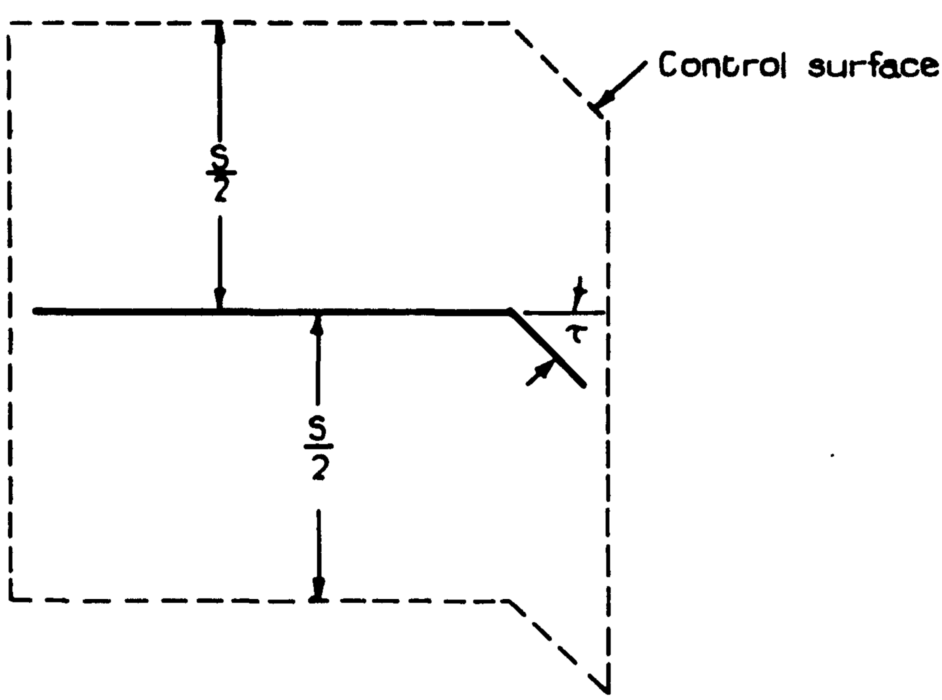

Figs. 3a & 3b.

Fig. 3a.

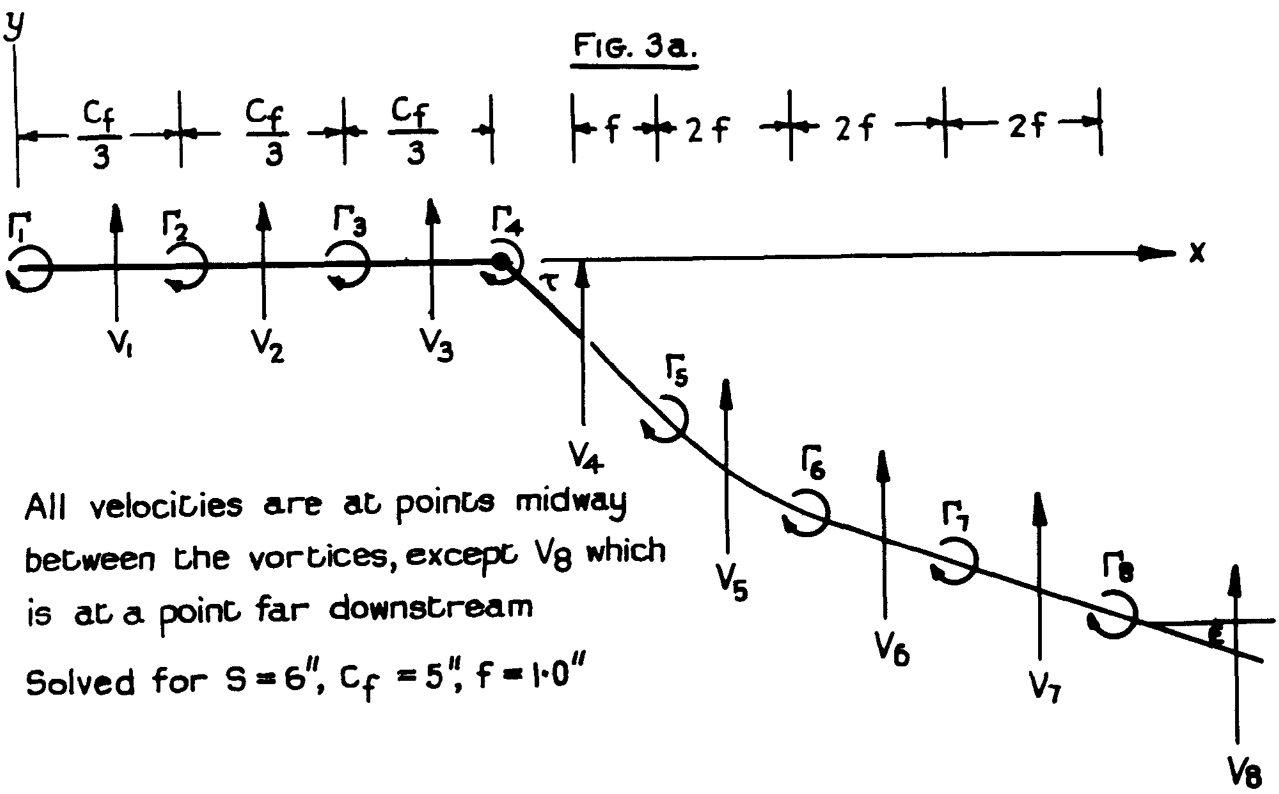

Fig. 3b.

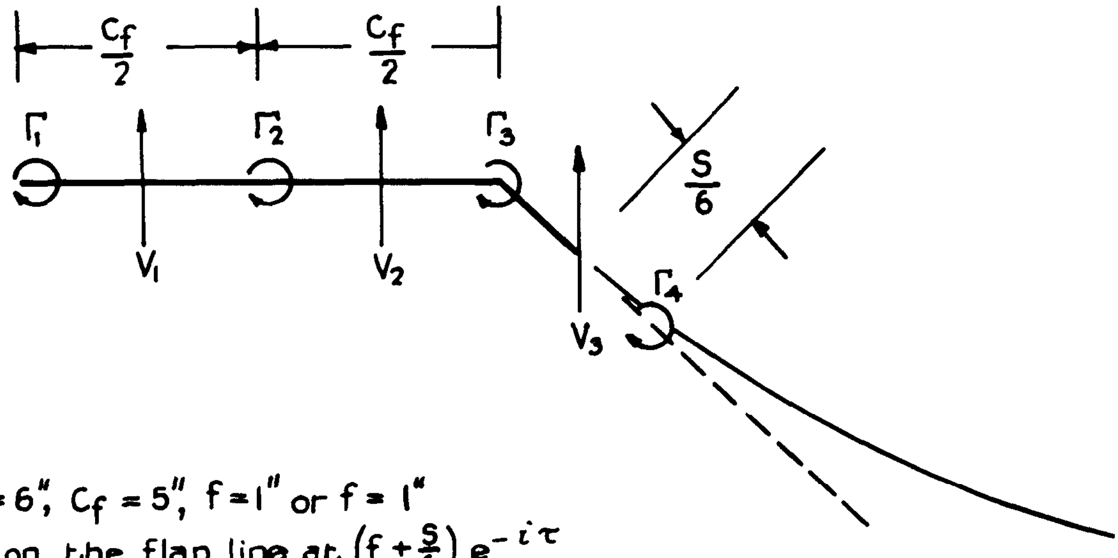

$S = 6''$, $C_f = 5''$, $f = 1''$ or $f = 1''$

Γ_4 on the flap line at $\left(f + \frac{S}{6}\right) e^{-i\tau}$

FIG. 4a.

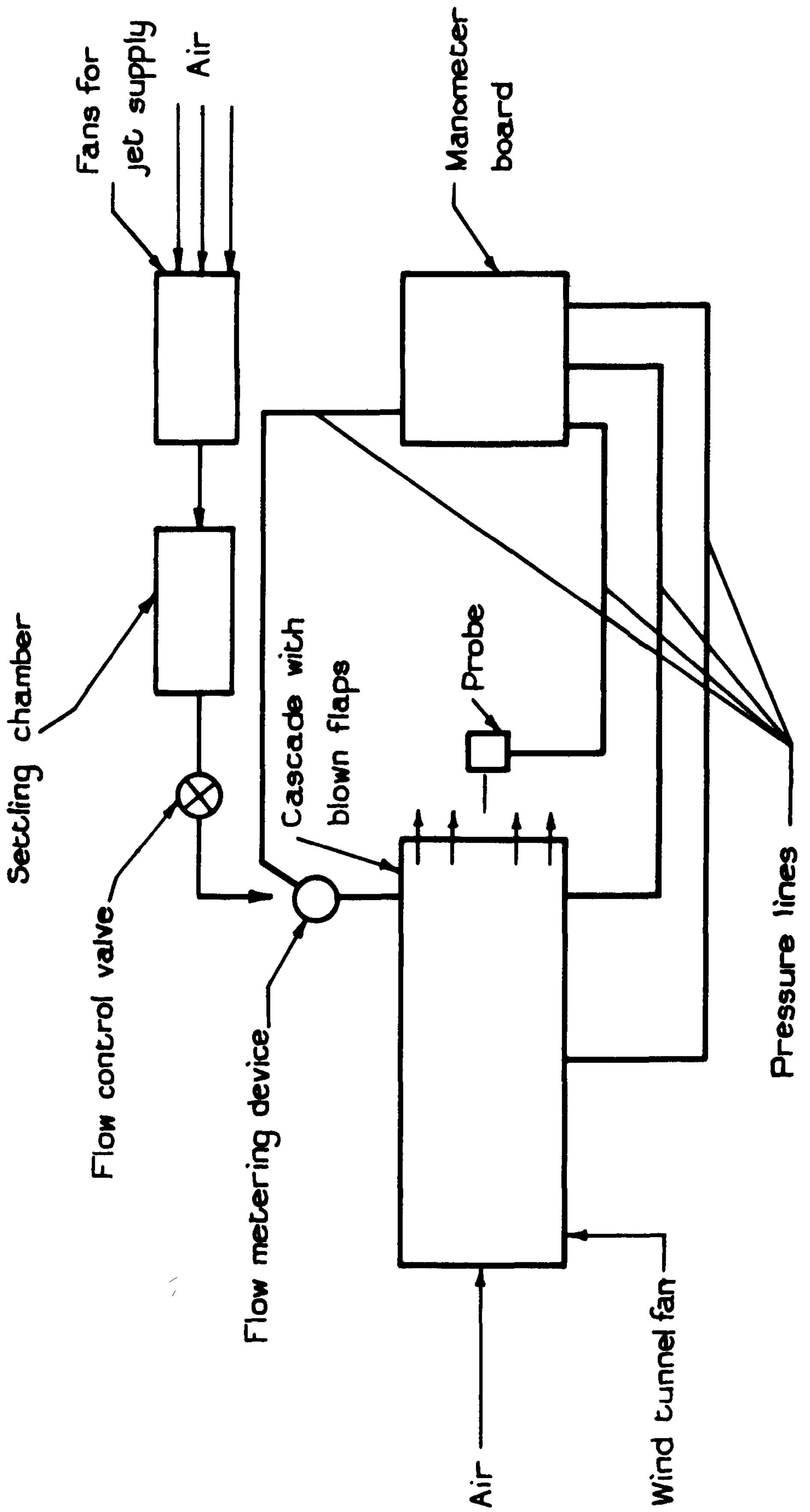

Fans for jet supply
Air
Settling chamber
Flow control valve
Flow metering device
Cascade with blown flaps
Probe
Manometer board
Pressure lines
Air
Wind tunnel fan

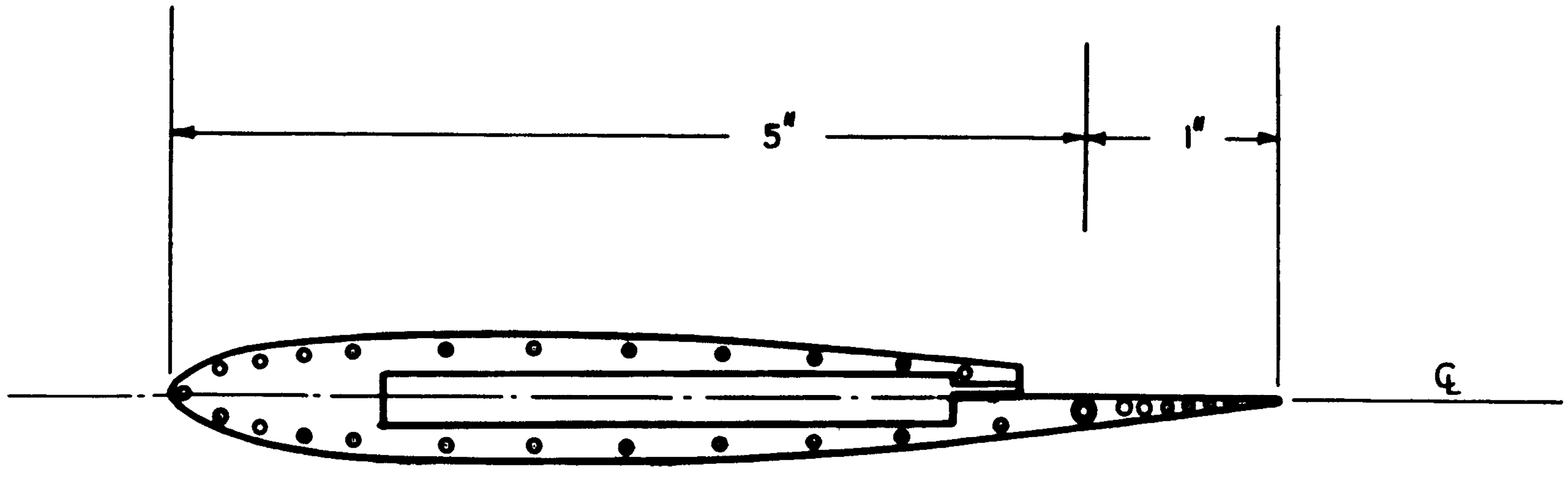

FIG. 4b.

Cascade blade fitted with blown flap – full size.

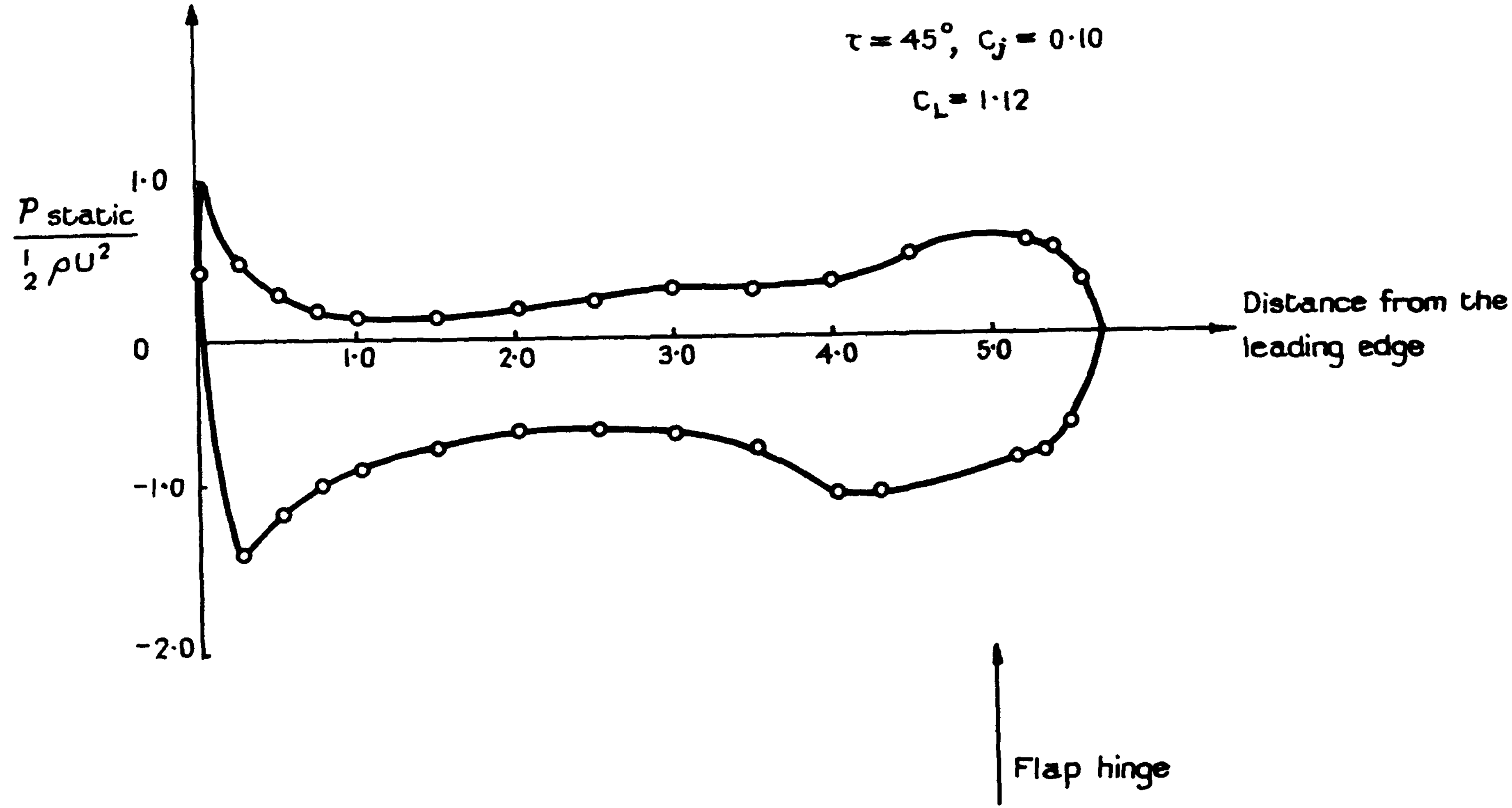

τ = 45°, Cj = 0·10
CL = 1·12
P static / ½ ρU²
1·0
0
-1·0
-2·0
1·0
2·0
3·0
4·0
5·0
Distance from the leading edge
Flap hinge

FIG. 5.

FIG. 6.

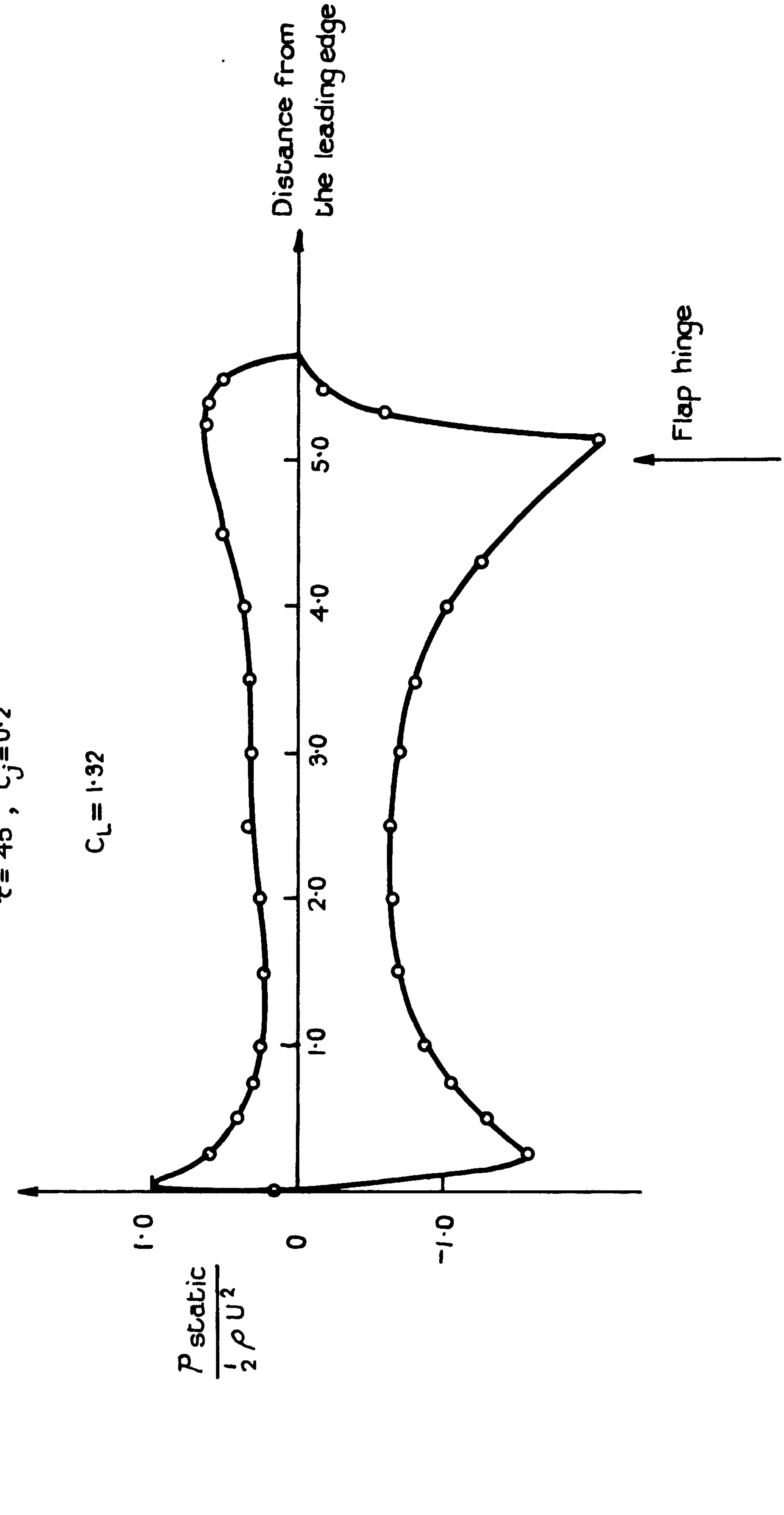

$\tau = 45°$, $C_j = 0{\cdot}2$
$C_L = 1{\cdot}32$
Distance from the leading edge
Flap hinge
$\frac{P_{static}}{\frac{1}{2}\rho U^2}$
1·0
0
-1·0
1·0
2·0
3·0
4·0
5·0

Fig. 7.

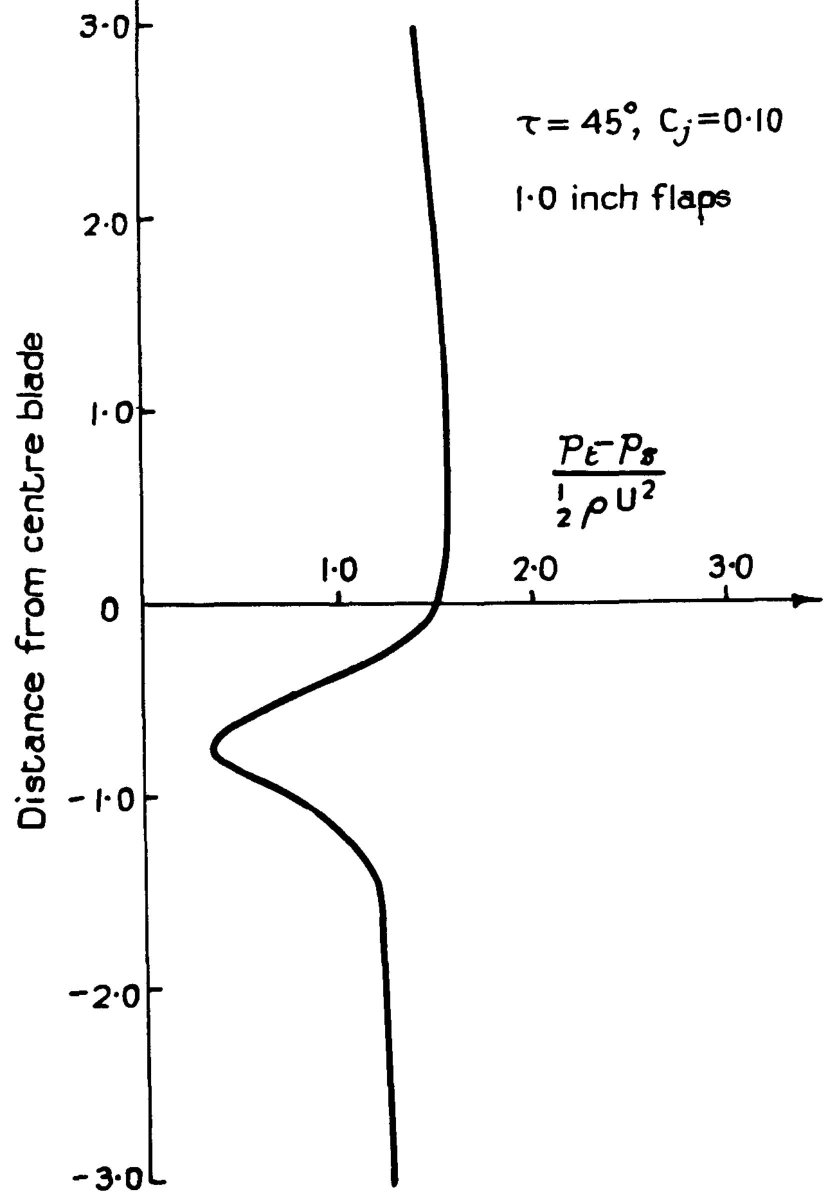

$\tau = 45°$, $C_j = 0.10$
1·0 inch flaps
$\frac{P_t - P_s}{\frac{1}{2}\rho U^2}$
1·0
2·0
3·0
3·0
2·0
1·0
0
-1·0
-2·0
-3·0
Distance from centre blade

Fig. 8.

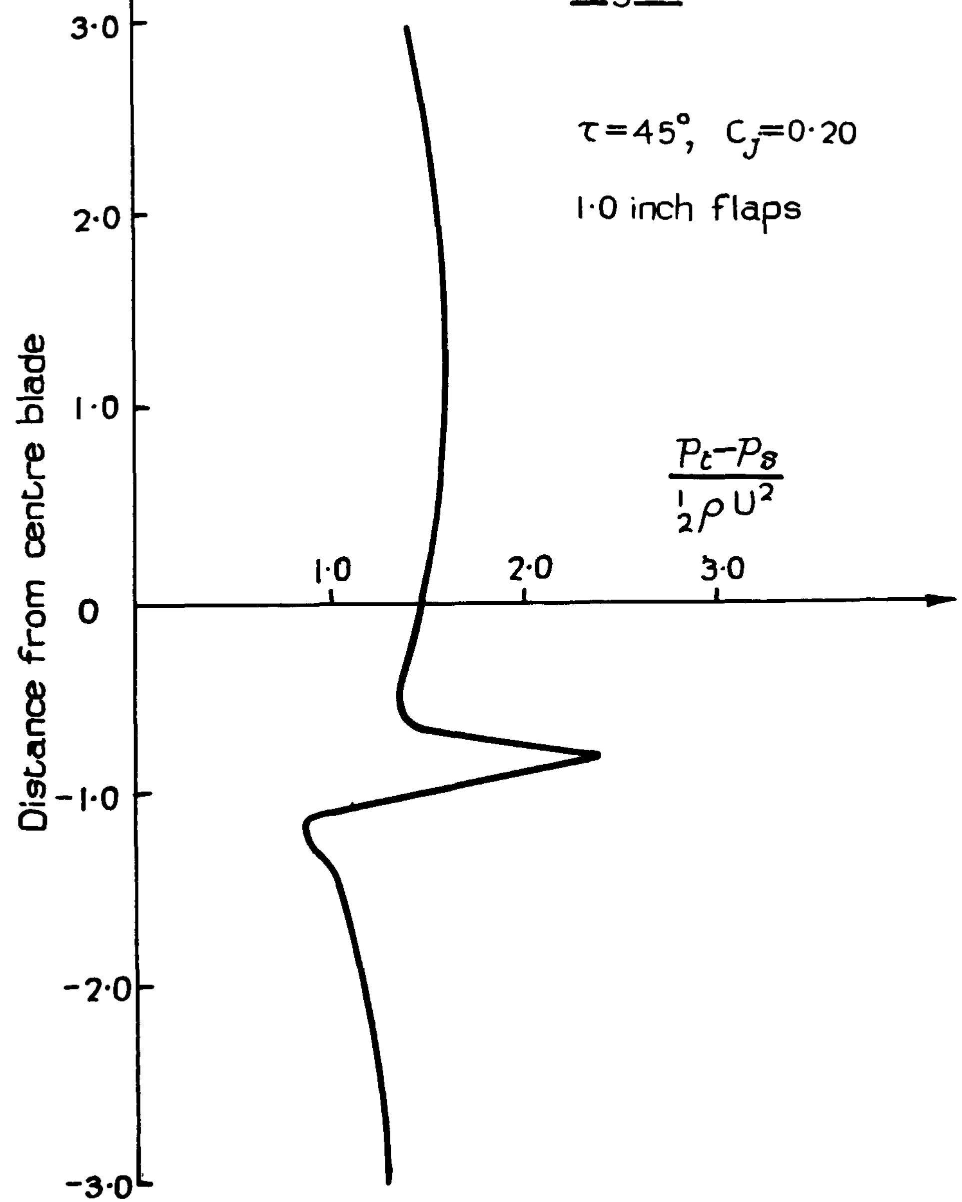

$\tau = 45°$, $C_j = 0.20$
1·0 inch flaps
$\frac{P_t - P_s}{\frac{1}{2}\rho U^2}$
1·0
2·0
3·0
3·0
2·0
1·0
0
-1·0
-2·0
-3·0
Distance from centre blade

Fig. 10.

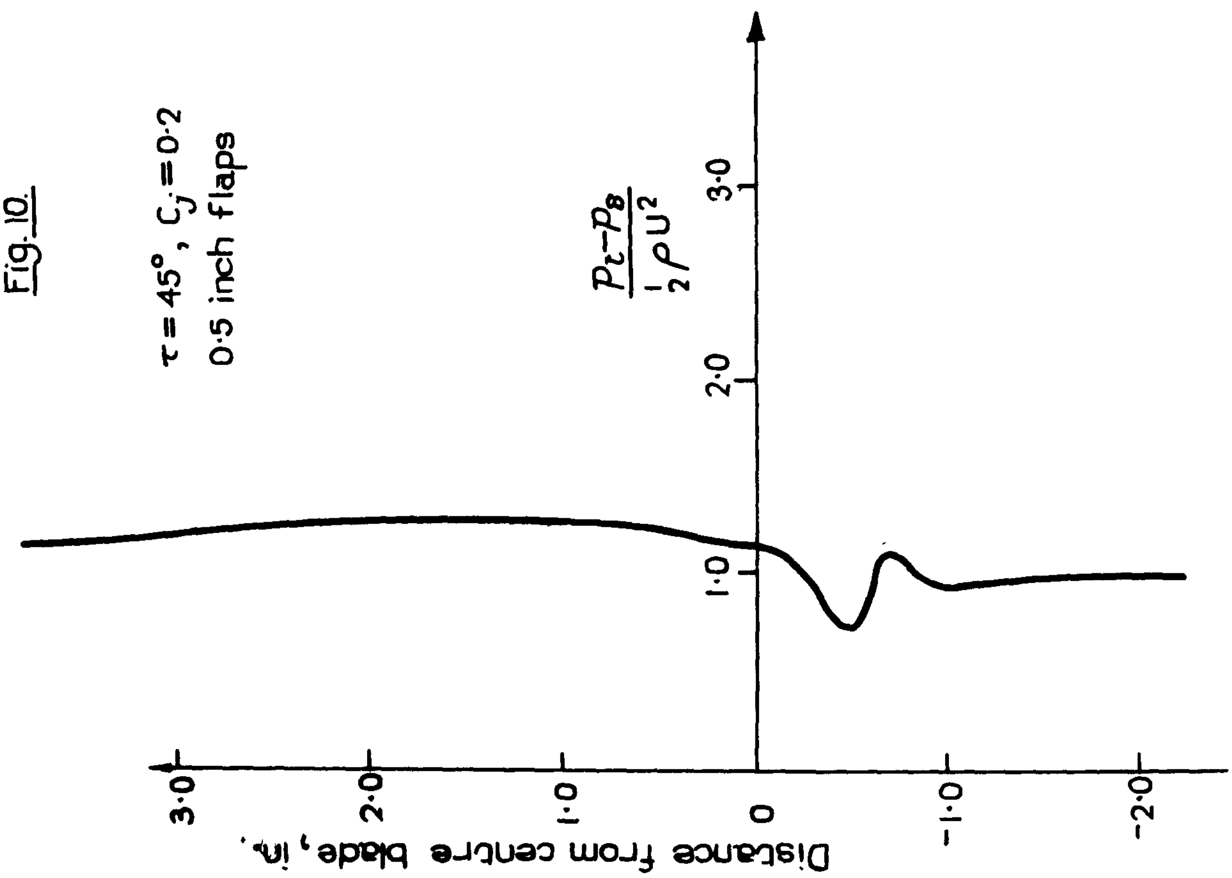
τ = 45°, Cj = 0·2
0·5 inch flaps
(Pt − PB) / ½ρU²
1·0
2·0
3·0
3·0
2·0
1·0
0
−1·0
−2·0
Distance from centre blade, in.

Fig. 9.

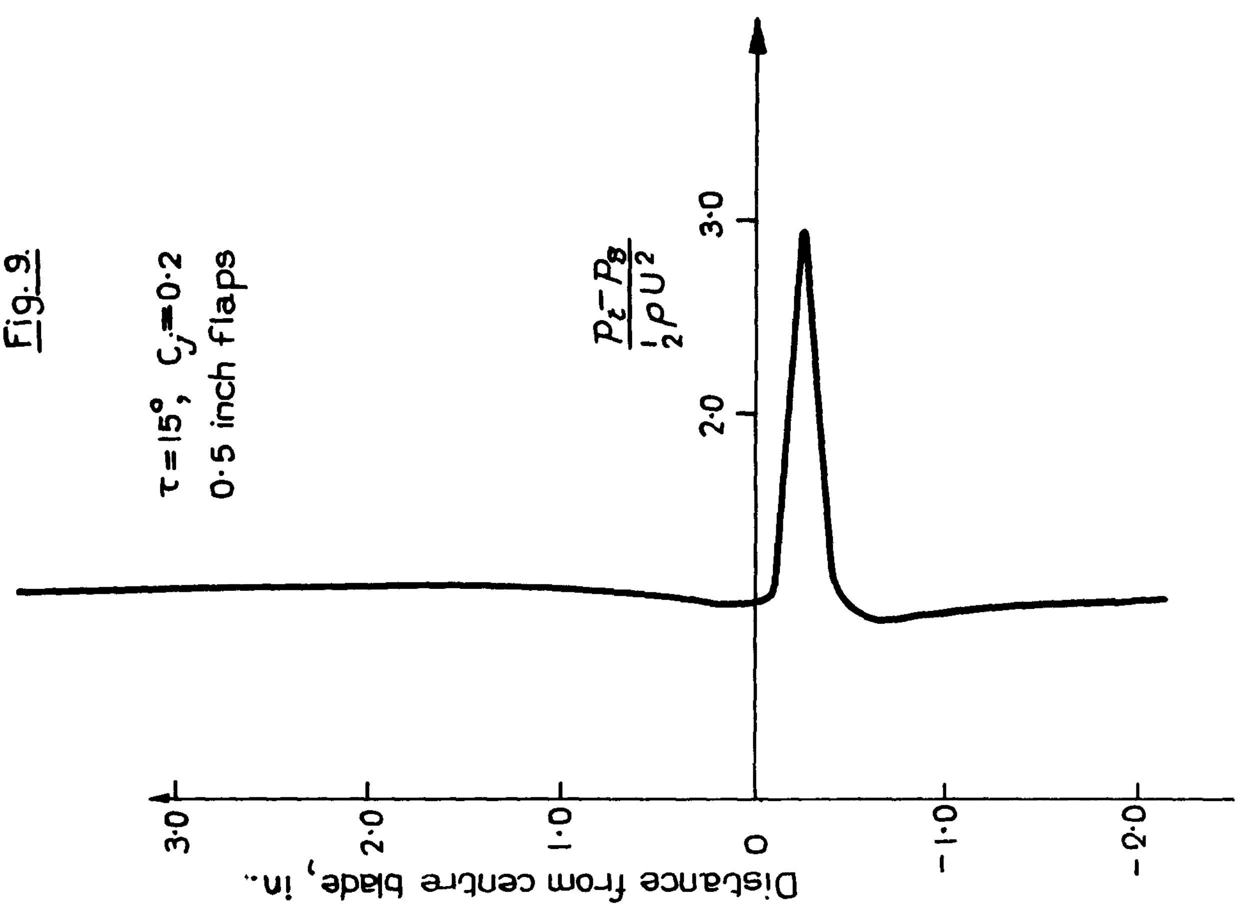
τ = 15°, Cj = 0·2
0·5 inch flaps
(Pt − PB) / ½ρU²
2·0
3·0
3·0
2·0
1·0
0
−1·0
−2·0
Distance from centre blade, in.

FIG. 11.

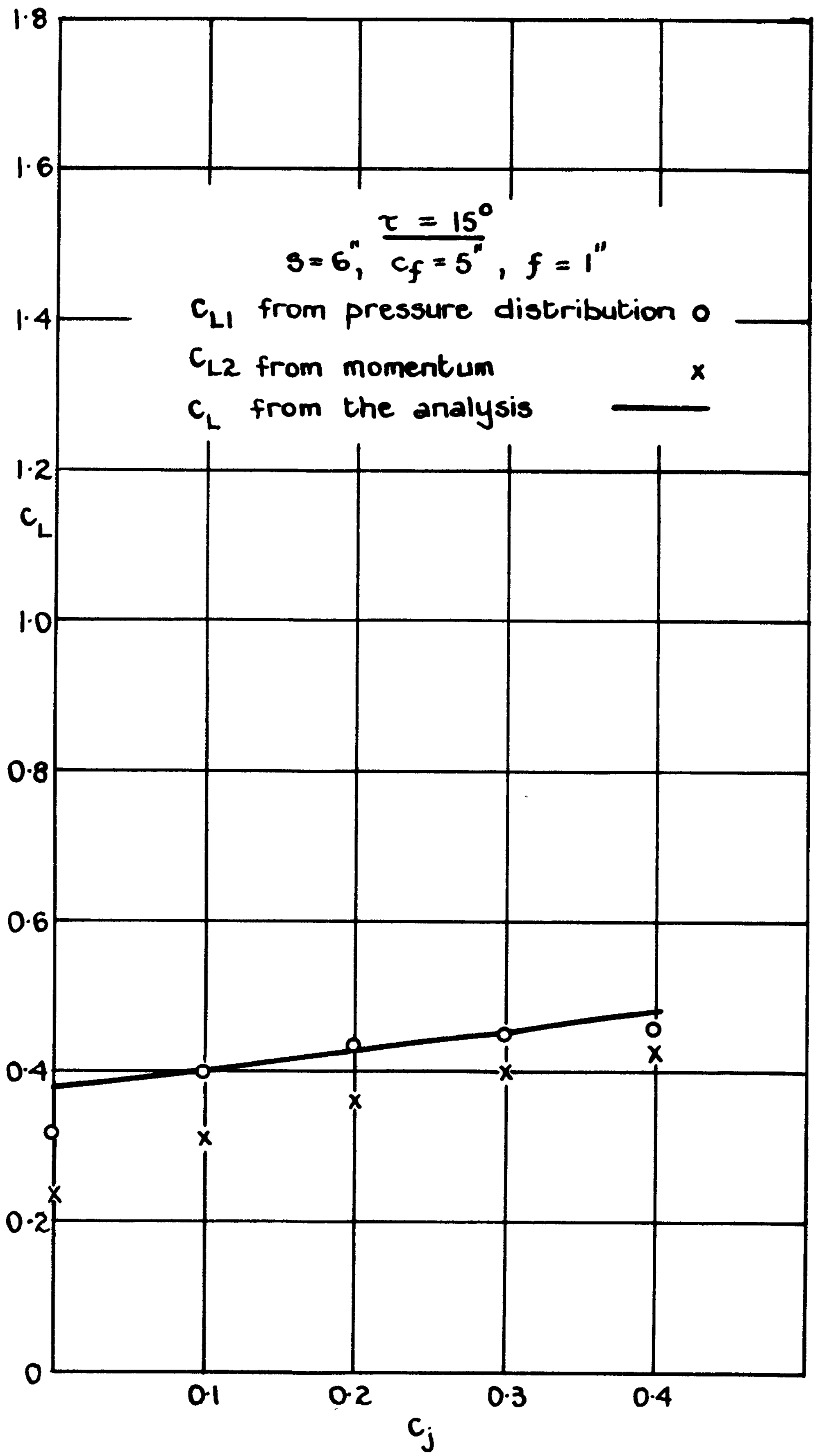

τ = 15°
s = 6", c_f = 5", f = 1"
C_L1 from pressure distribution o
C_L2 from momentum x
C_L from the analysis
1·8
1·6
1·4
1·2
C_L
1·0
0·8
0·6
0·4
0·2
0
0·1
0·2
0·3
0·4
C_j

FIG. 12.

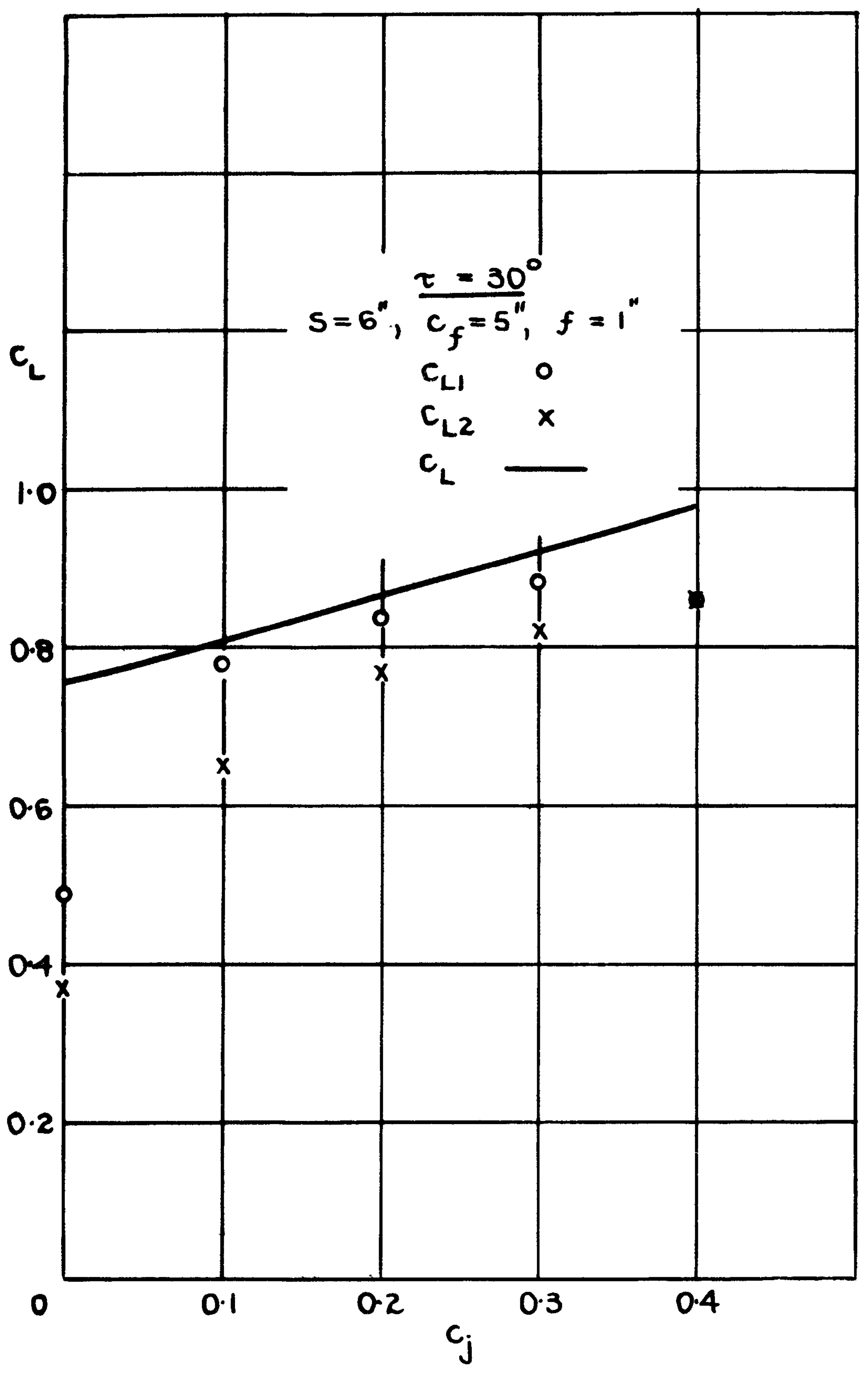

FIG. 13.

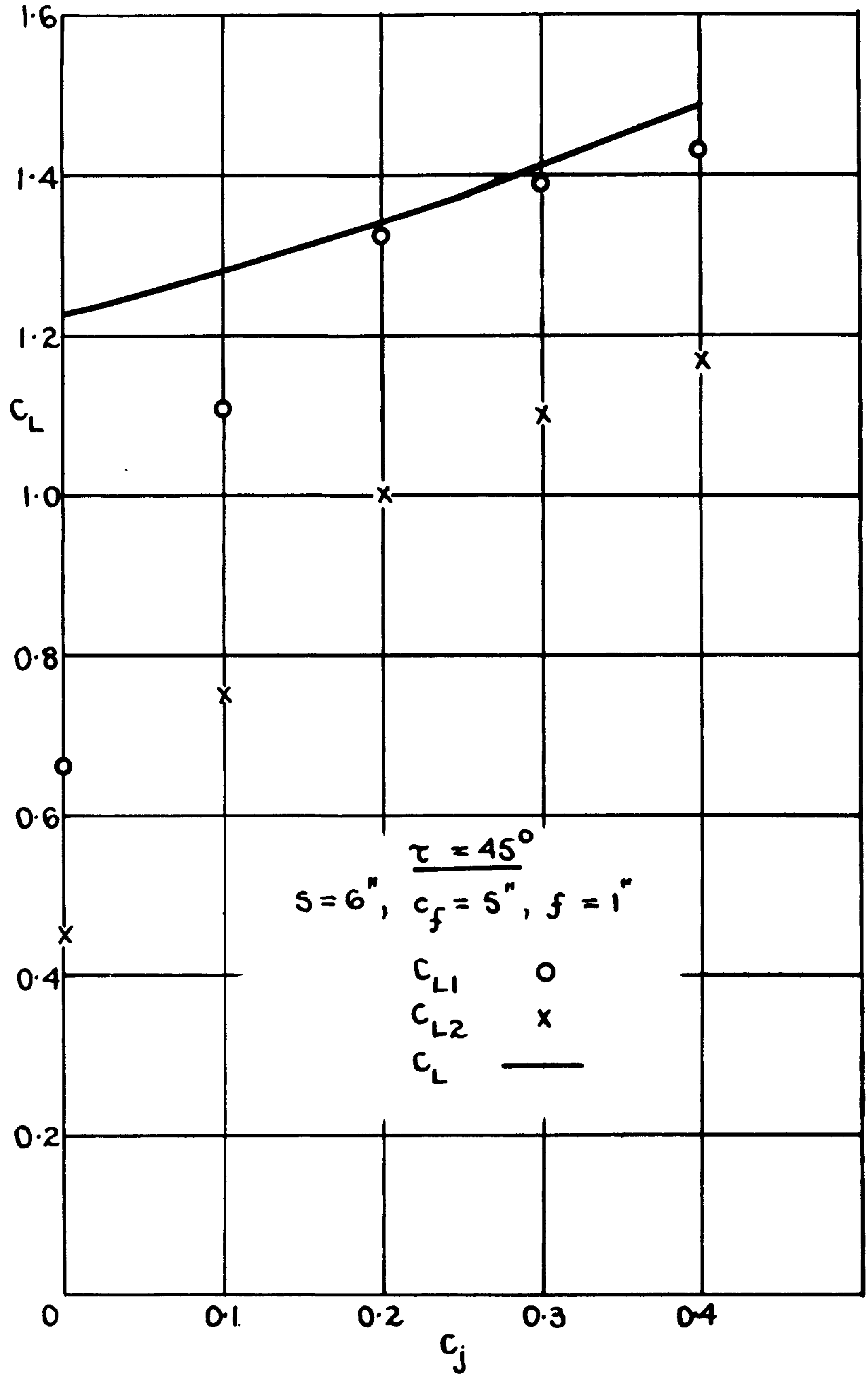

1·6
1·4
1·2
C_L
1·0
0·8
0·6
0·4
0·2
0
0·1
0·2
0·3
0·4
C_j
$\tau = 45°$
$S = 6''$, $c_f = 5''$, $f = 1''$
C_{L1} o
C_{L2} x
C_L ——

FIG. 14.

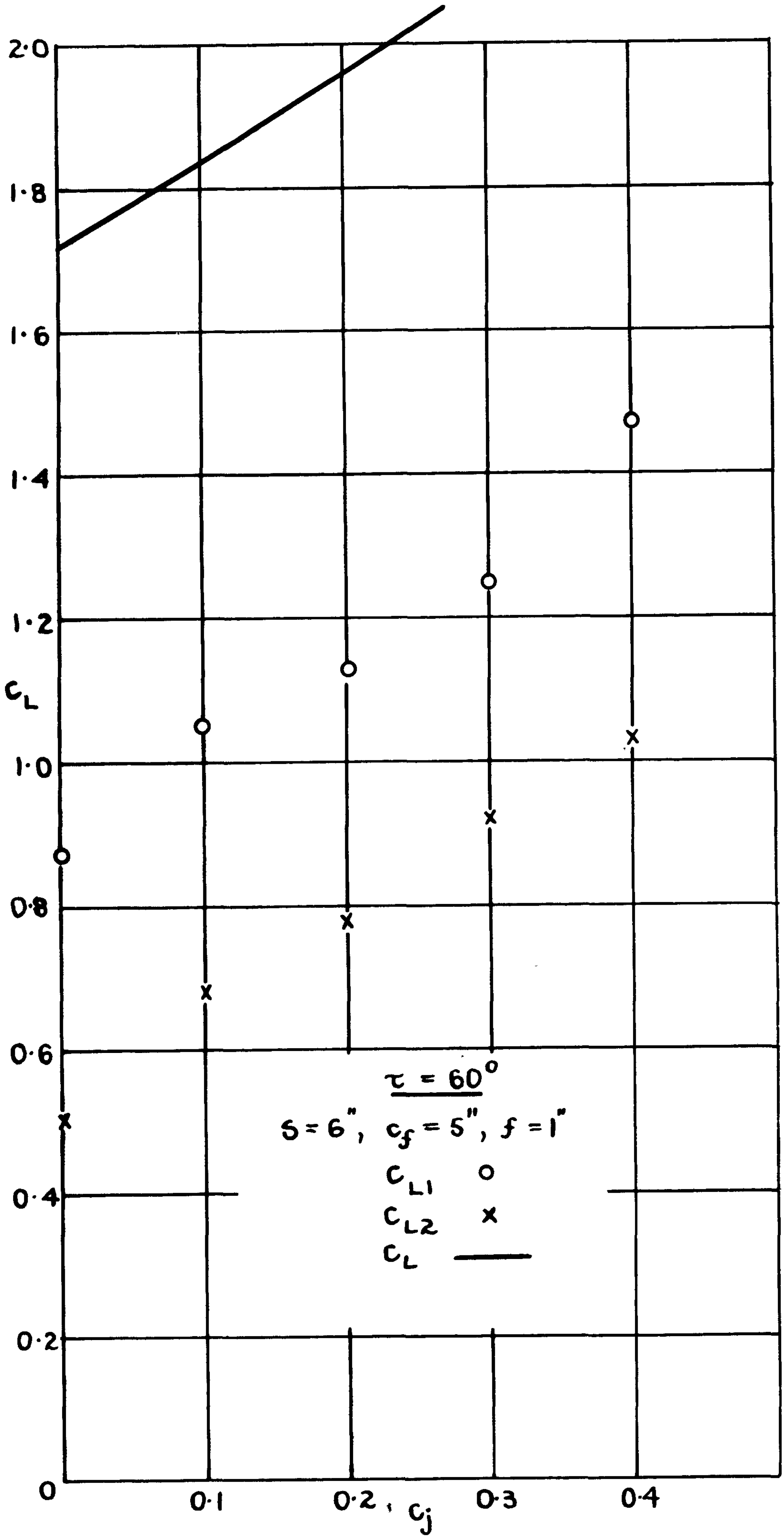
2·0
1·8
1·6
1·4
1·2
C_L
1·0
0·8
0·6
0·4
0·2
0
0·1
0·2
0·3
0·4
C_j
τ = 60°
S = 6", c_f = 5", f = 1"
C_{L1} o
C_{L2} x
C_L

Fig 15

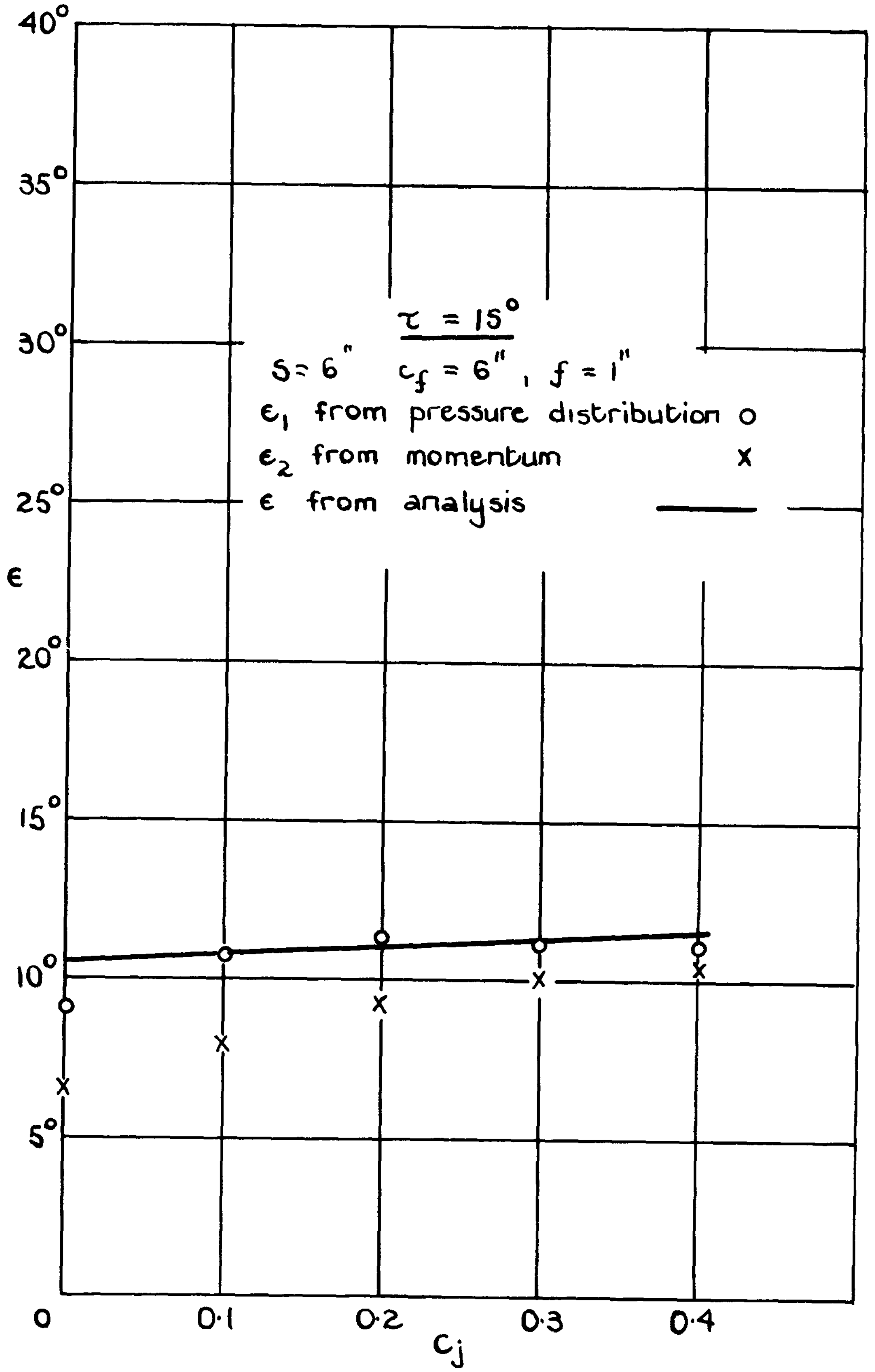

40°
35°
30°
25°
20°
15°
10°
5°
0
ε
$\tau = 15°$
$S = 6''$ $c_f = 6''$, $f = 1''$
ϵ_1 from pressure distribution o
ϵ_2 from momentum x
ϵ from analysis
0·1
0·2
0·3
0·4
C_j

FIG. 16.

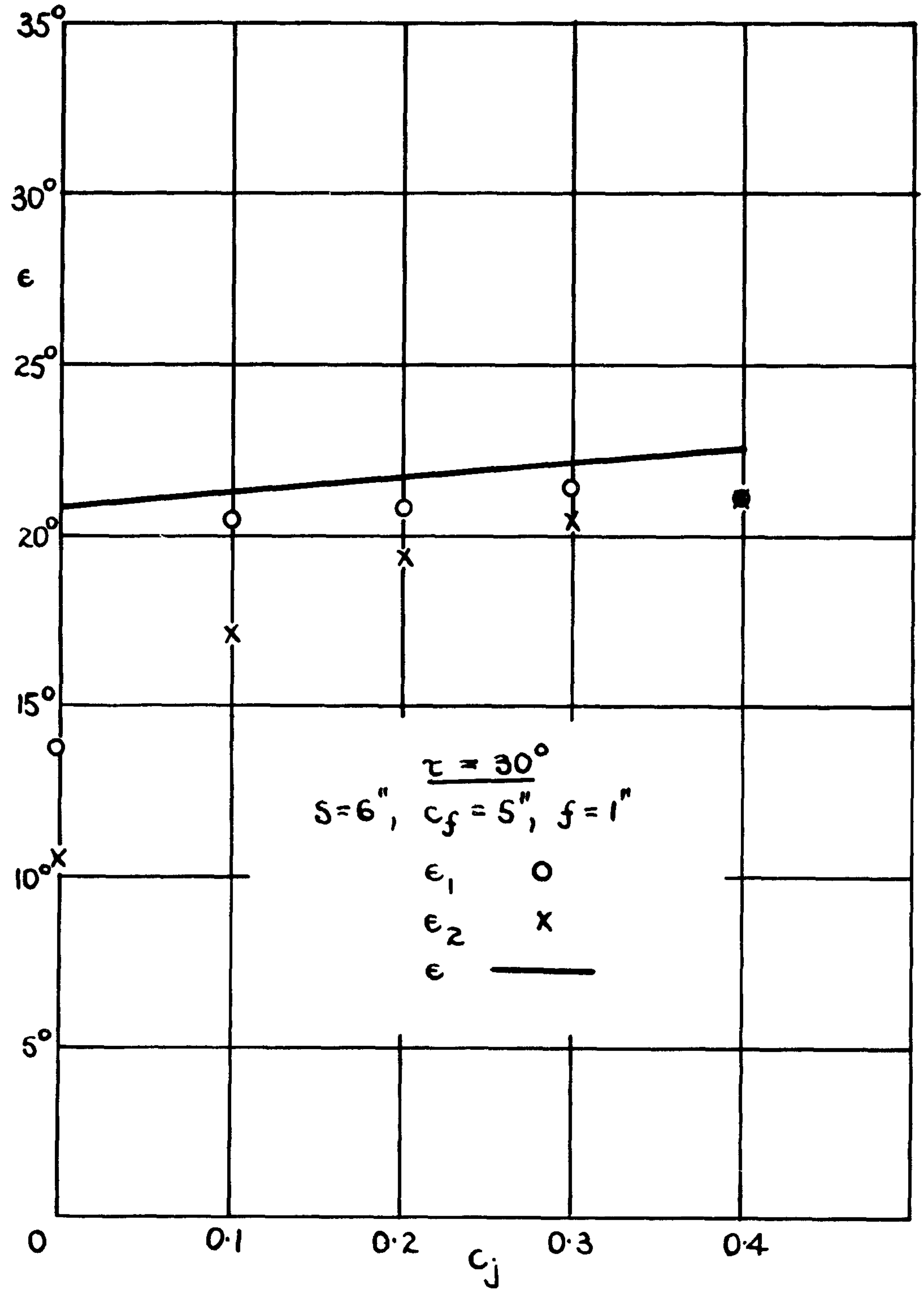

FIG. 17.

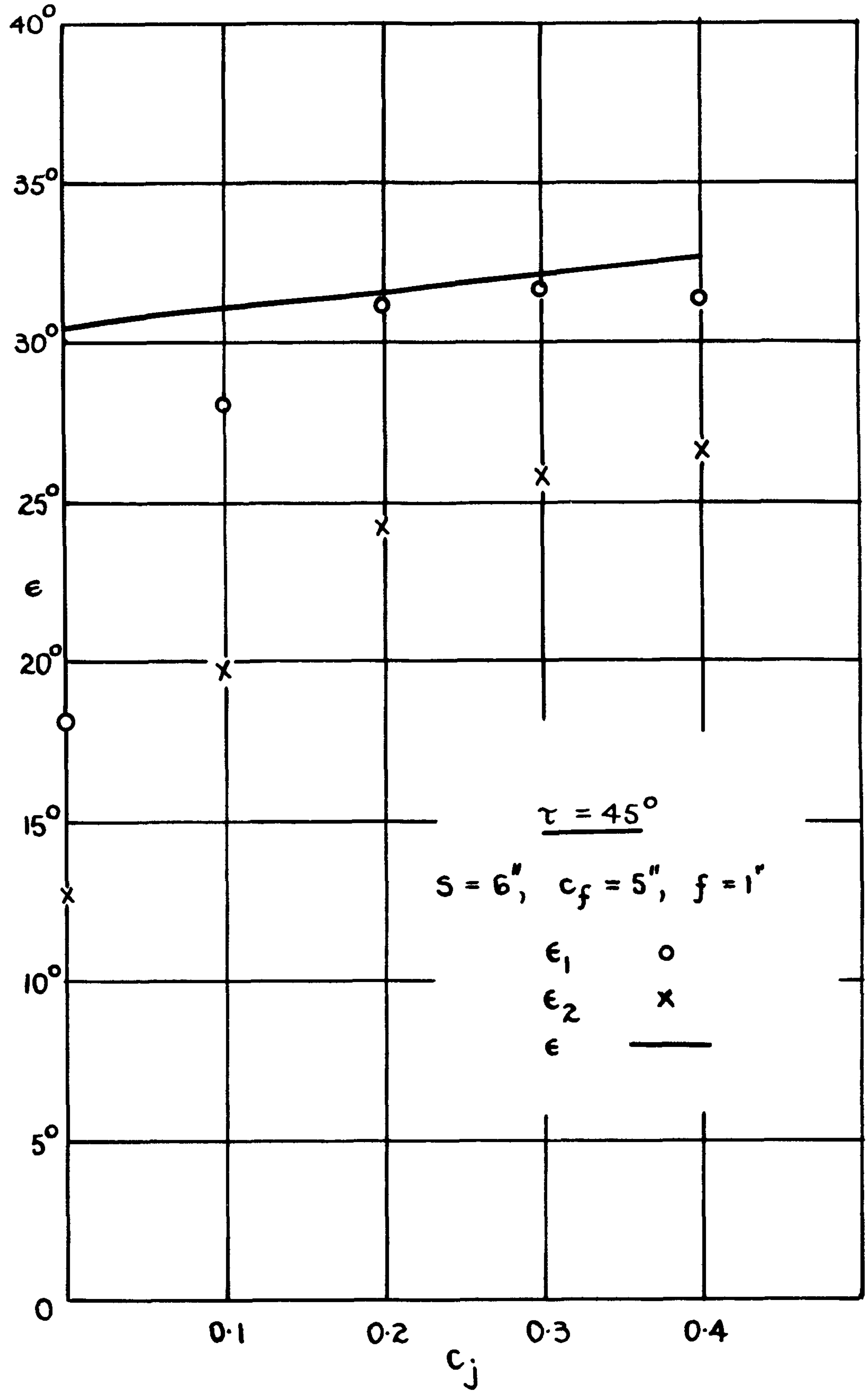
40°
35°
30°
25°
20°
15°
10°
5°
0
ε
0·1
0·2
0·3
0·4
c_j
τ = 45°
S = 6", c_f = 5", f = 1"
ϵ_1 o
ϵ_2 x
ε

FIG. 18.

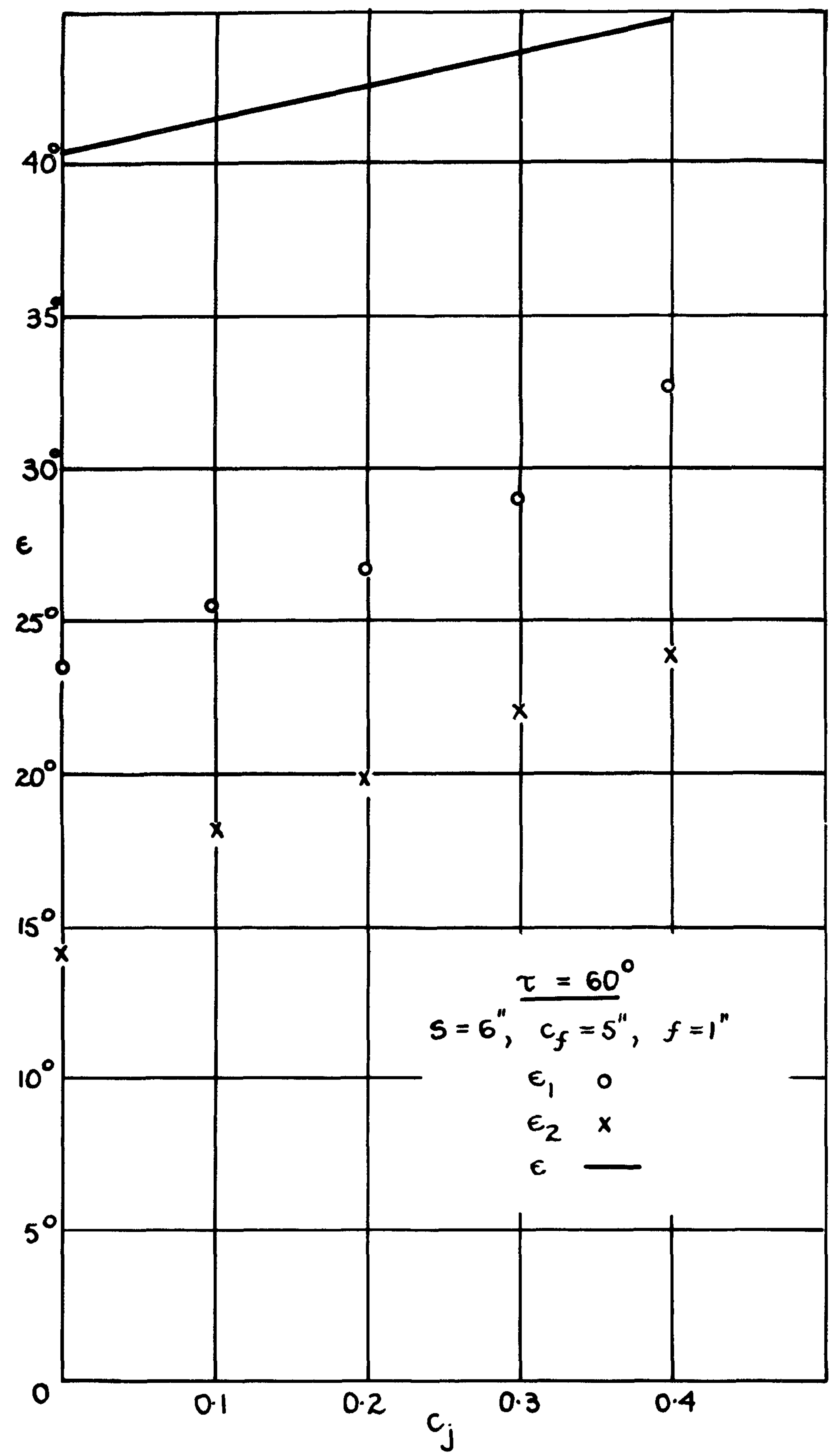

40°
35°
30°
25°
20°
15°
10°
5°
0
ε
0·1
0·2
0·3
0·4
c_j
τ = 60°
S = 6", c_f = 5", f = 1"
ϵ_1 o
ϵ_2 x
ε ——

Fig. 19

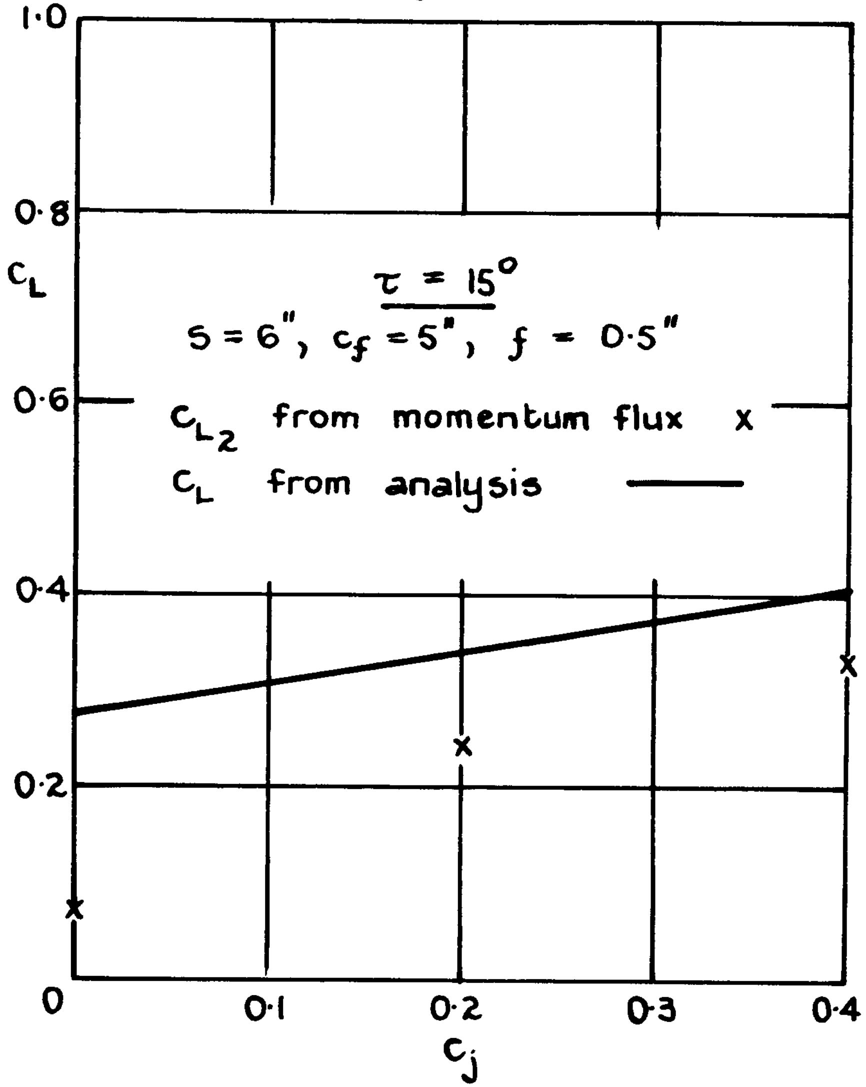
1·0
0·8
0·6
0·4
0·2
0
C_L
$\tau = 15^\circ$
$s = 6''$, $c_f = 5''$, $f = 0{\cdot}5''$
C_{L_2} from momentum flux x
C_L from analysis
0·1
0·2
0·3
0·4
C_j

Fig. 20

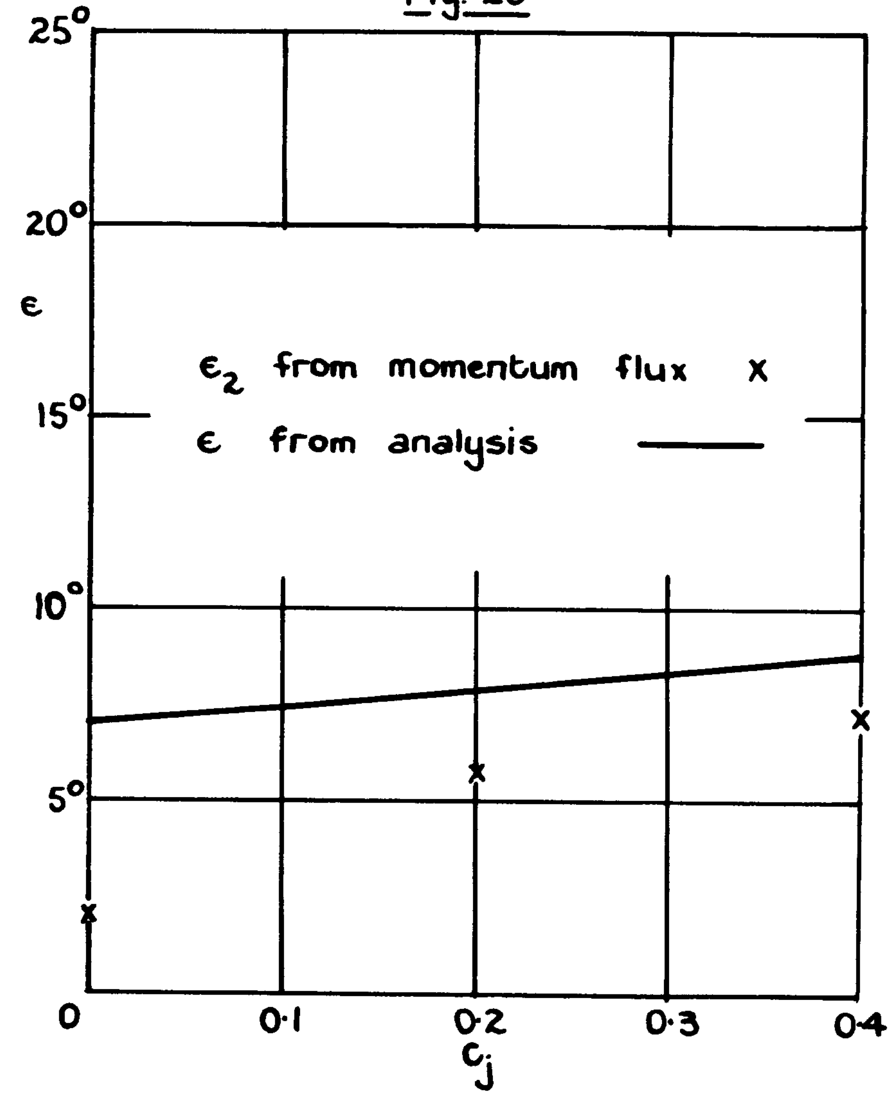
25°
20°
15°
10°
5°
0
ϵ
ϵ_2 from momentum flux x
ϵ from analysis
0·1
0·2
0·3
0·4
C_j

FIG. 21.

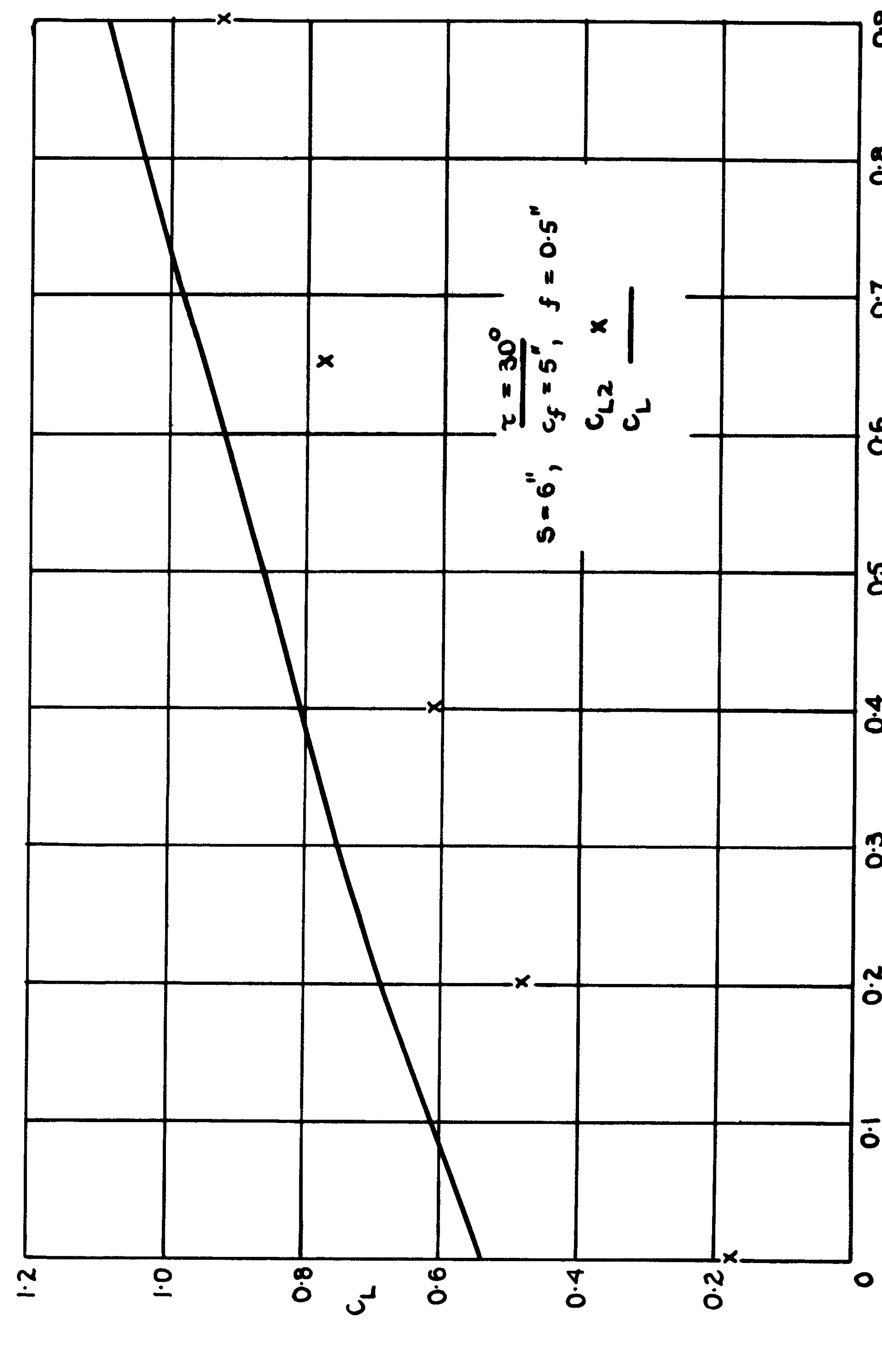

S = 6", τ = 30°, c_f = 5", f = 0.5"
C_L2 x
C_L —
C_j
C_L
0
0·1
0·2
0·3
0·4
0·5
0·6
0·7
0·8
0·9
0·2
0·4
0·6
0·8
1·0
1·2

FIG. 22.

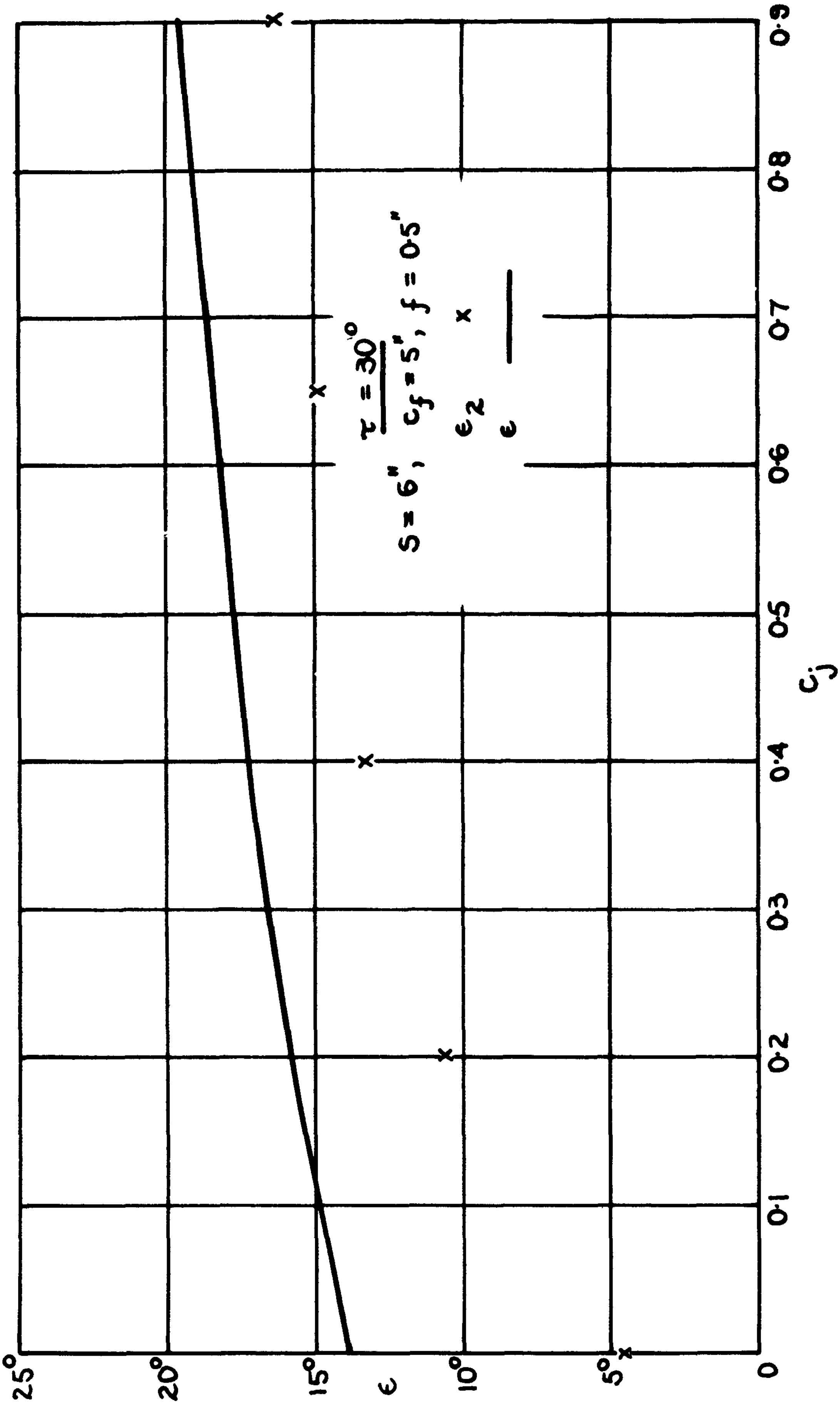

FIG. 23

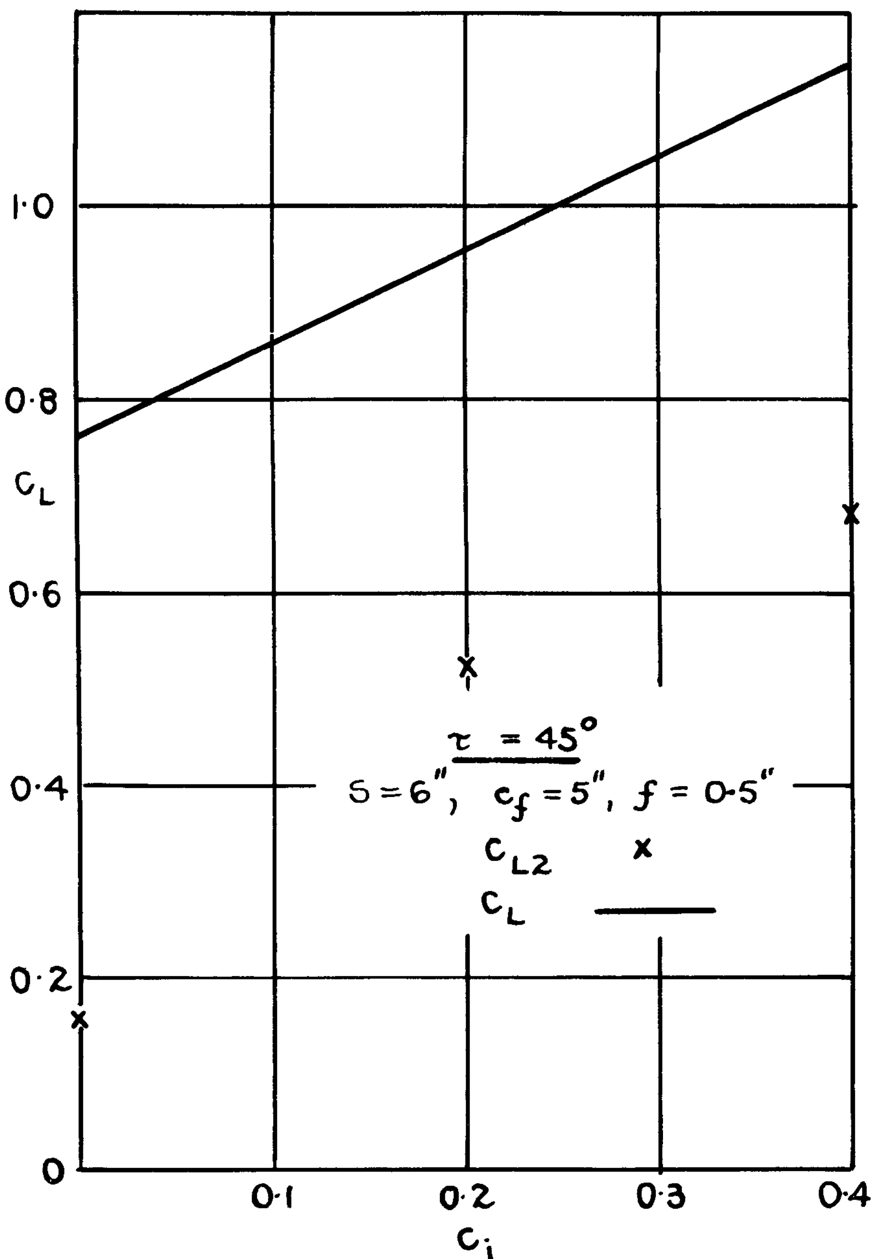

FIG. 24.

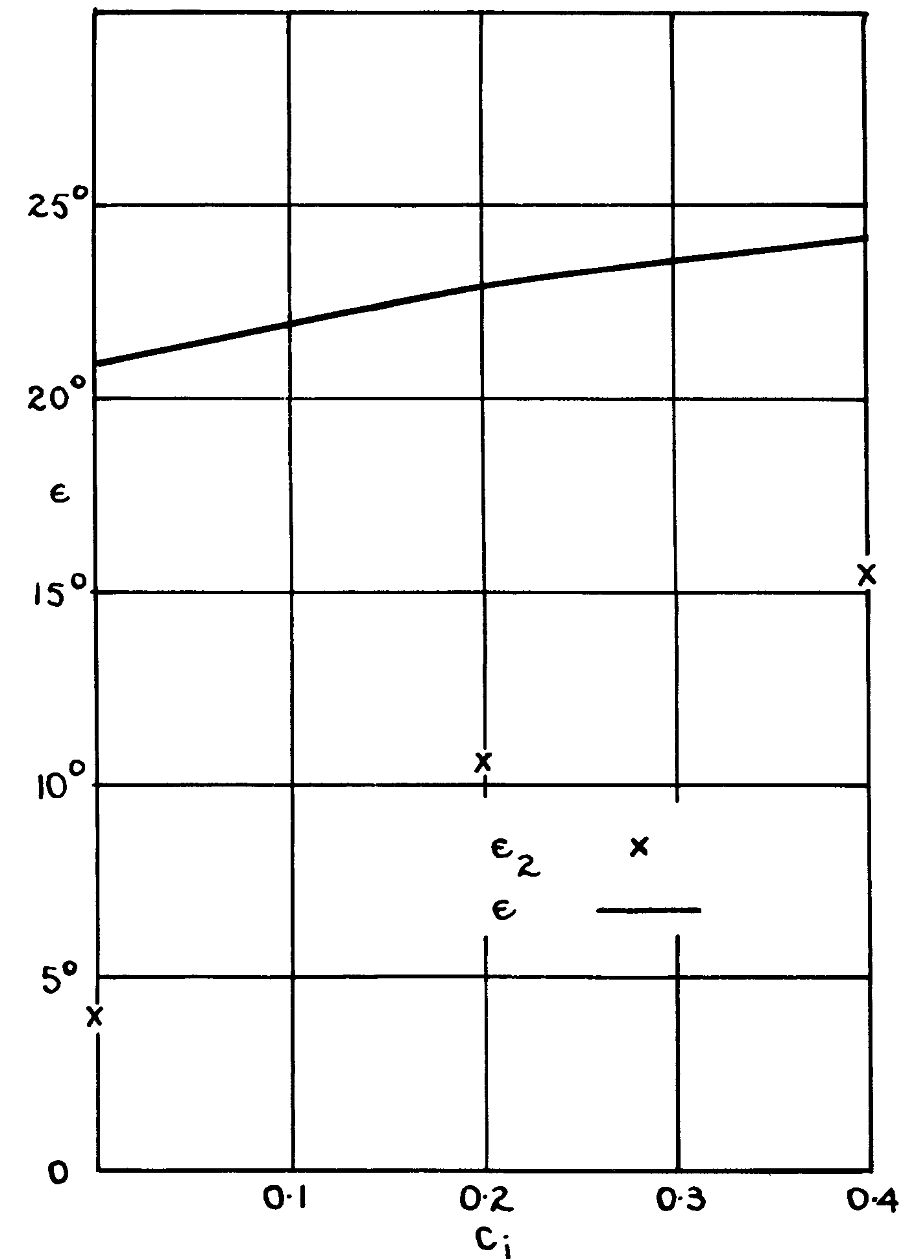

DS83720/1 Wt60 K4 12/60 CL

C.P. No. 526
23.6.59
Kruger, R. A., Marsh, H. and
Horlock, J. H. - Univ. of Cambridge.

THE PERFORMANCE OF A CASCADE FITTED WITH BLOWN FLAPS

The performance of a compressor with a cascade of inlet guide vanes fitted with blown flaps has been investigated. A series of experiments has been made with a cascade of uncambered blades fitted with blown flaps. The results are compared with an analytical method for estimating the performance of a cascade of blades fitted with blown flaps.

C.P. No. 526
23.6.59
Kruger, R. A., Marsh, H. and
Horlock, J. H. - Univ. of Cambridge.

THE PERFORMANCE OF A CASCADE FITTED WITH BLOWN FLAPS

The performance of a compressor with a cascade of inlet guide vanes fitted with blown flaps has been investigated. A series of experiments has been made with a cascade of uncambered blades fitted with blown flaps. The results are compared with an analytical method for estimating the performance of a cascade of blades fitted with blown flaps.

C.P. No. 526
23.6.59
Kruger, R. A., Marsh, H. and
Horlock, J. H. - Univ. of Cambridge.

THE PERFORMANCE OF A CASCADE FITTED WITH BLOWN FLAPS

The performance of a compressor with a cascade of inlet guide vanes fitted with blown flaps has been investigated. A series of experiments has been made with a cascade of uncambered blades fitted with blown flaps. The results are compared with an analytical method for estimating the performance of a cascade of blades fitted with blown flaps.

C.P. No. 526

Printed and published by
HER MAJESTY'S STATIONERY OFFICE

To be purchased from
York House, Kingsway, London w.c.2
423 Oxford Street, London w.1
13A Castle Street, Edinburgh 2
109 St. Mary Street, Cardiff
39 King Street, Manchester 2
50 Fairfax Street, Bristol 1
2 Edmund Street, Birmingham 3
80 Chichester Street, Belfast 1
or through any bookseller

Printed in England

S.O. Code No. 23-9012-26

C.P. No. 526